Enhancement of nitrate removal and recovery from municipal wastewater through single- and multi-batch electrodialysis: Process optimisation and energy consumption

Mohammadi Rubaba, Ramasamy Deepika Lakshmi, Sillanpää Mika

DOI: 10.1016/j.desal.2020.114726

Enhancement of nitrate removal and recovery from municipal wastewater through single- and multi-batch electrodialysis: Process optimisation and energy consumption

Rubaba Mohammadi [a *], Deepika Lakshmi Ramasamy [a], Mika Sillanpää [b,c,d,e]

[a]*Department of Separation Science, Lappeenranta-Lahti University of Technology, Sammonkatu 12, FI-50130 Mikkeli, Finland.*

[b] *Institute of Research and Development, Duy Tan University, Da Nang 550000, Vietnam.*

[c] *Faculty of Environment and Chemical Engineering, Duy Tan University, Da Nang 550000, Vietnam.*

[d] *School of Civil Engineering and Surveying, Faculty of Health, Engineering and Sciences, University of Southern Queensland, West Street, Toowoomba, 4350 QLD, Australia.*

[e] *Department of Chemical Engineering, School of Mining, Metallurgy and Chemical Engineering, University of Johannesburg, P. O. Box 17011, Doornfontein 2028, South Africa.*

[f] *School of Engineering Science, Lappeenranta-Lahti University of Technology, Lappeenranta 53851, Finland.*

[*]Corresponding author: Rubaba.Mohammadi@lut.fi, ru.mohammadi@ymail.com

Abstract

The vast volume of nutrients discharging from municipal wastewater (MWW) into water resources, along with the stringent limitations of their discharge, can be addressed via the recovery of nutrients from this stream. Hence, the purpose of this study is to optimise and enhance nitrate recovery from MWW using single and two-stage electrodialysis processes. Furthermore, the chemical quality of the recycled water was comprehensively tested and compared with the standards. Better nitrate recovery was obtained at the flow rate of 60 Lh^{-1}, with four cell pairs, diluted-to-concentrated volume ratio (*VD/VC*) of 2/0.5 and using Na_2SO_4 as the electrolyte. Under these conditions, the nitrate concentration in the diluted part was near zero with a concentration ratio of 4.6 and energy consumption of 1.44 kWh kg NO_3^-. Two-stage batch electrodialysis enhanced nitrate concentration ratio to 19.2 with energy consumption of 4.34 kWh kg NO_3^-. The volumes of 2 L and 8 L of water could be recovered per 0.5 L of concentrated solution by applying single- and two-stage batch electrodialysis respectively. The pH, permeation sequence, membrane fouling and water transfer were also investigated. These results indicated that the electrodialysis system has the potential to provide functional nutrient recovery and drinking water source alternatives.

Keywords: *electrodialysis, energy, nitrate recovery, nutrient, water recovery*

1. Introduction

Increasing demands for food and water have resulted from a remarkable increase in the global population, thereby exerting high pressure on the accessibility of water and food resources. An increase of 70% in agricultural demand and 55% in global water demand is anticipated by 2050 [1]. Food suppliers and farmers require a considerable amount of fertiliser, and concerns about the long-term availability of natural fertilisers is increasing [2]. One of the main components of fertiliser is nitrate. Nitrate is a highly water-soluble ion, so its discharge from wastewater or fertiliser to ground or surface water imposes a severe threat to drinking water supplies and promoting eutrophication [[3],[4]]. Just 40% of reactive nitrogen accumulates in crops, the rest is lost through water and air pathways, affecting human health, the quality of water and air, and biodiversity [[1],[2]]. On the subject of air pollution, the US Environmental Protection Agency estimated that there are 0.48 million tons of nitrous oxide emissions from agricultural activities in the US annually, which is about 80% of total US nitrous oxide emissions from agriculture and about 10% of the worldwide nitrous oxide emissions from agriculture [5]. The nitrous oxide contributes directly to the generation of excessive ozone in a short time and the reduction of atmospheric carbon dioxide sequestration over a longer time. Besides this, both nitrogen oxide and ammonia also react with other atmospheric constituents to form aerosols and air pollution [6]. Hence, the problems associated with the excess loading into water resources and the atmosphere, and demand for nitrogen can be reduced through nitrate recovery, consequently prompting a greener and purer environment [2]. Recently, wastewater streams have been perceived as a promising source for the recovery of energy and water, as well as nitrate [2]. However, most wastewater treatment plants, and consequently the related technologies, have been designed based on nitrate removal, not nitrate capture or recovery. Some of the methods that can be used for nitrate recovery from domestic wastewater include chemical precipitation [[2],[7]], ion exchange (IX) [[2],[7],[8],[9]], adsorption [10], and using

a pressure-driven membrane, such as in nanofiltration (NF), reverse osmosis (RO), membrane distillation (MD) and forward osmosis (FO) [[11],[12],[13]]. There are a few pros and cons to each of these technologies. For instance, a significant drawback related to the chemical precipitation process is the increase in the production of sludge (35% on a v/v basis), mainly when using alum-based or lime-based precipitation [[2],[14],[11]]. IX requires additional chemical regeneration during the operation. A high regenerate chemical concentration and high operational costs are expected in order to treat highly polluted waste streams[11]. Pressure-driven membranes have demonstrated enormous potential for nutrient recovery from wastewater. However, the formation of a polarisation film, fouling and high energy demand are limiting factors [[15],[16]]. Along this line, electrodialysis (ED) is considered to be an energy-efficient process. It has proven to be advantageous over conventional RO in the case of a desalination process with a low salt concentration[17].

Briefly, the ED process involves the separation and concertation of wastewater-derived ions by applying an electric field. An illustration showing the basic ED unit configuration is presented in **Fig. 1**. An ED unit typically consists of a series of alternating parallel anion exchange membranes (AEMs) and cation exchange membranes (CEMs), which are placed between anode and cathode. ED is based on the transport of ions by the application of an electric current/voltage in order to provide the driving force across ion-exchange membranes. As a result, electrically charged ions move: the cations move towards the cathode and the anions move towards the anode. Cations are transported across the CEMs, enter the concentrate compartment and are trapped by an AEMs. Similarly, the anions move from the dilute compartment to the concentrate compartment through AEMs and are trapped by the CEMs. Thus, the ions are stripped away in the dilute compartment while they are concentrated in the concentrate compartment [[27],[28],[29],[30]]. ED can be operated in continuous mode (one pass flow), feed and bleed mode (partial recirculation) and batch mode [18]. In a batch mode,

all feed, concentrate and electrode rinse solutions (electrolyte) are circulated during the process operation, resulting in a high desalination rate. ED can recover nutrients as a concentrated product while simultaneously producing clean water. ED is not an energy-intensive process and has no sludge production, and further, no regeneration chemicals are required compared with other recovery methods [17]. It can be used ranging from a very large scale to a very small scale, making it a feasible approach for small and remote communities [19].

However, in most cases, ED is used for the desalination of brackish water [[20],[21],[22],[23]], and few studies have reported ED being used for nutrient recovery from wastewater. Additionally, the majority of studies regarding the use of ED demonstrated nutrient recovery from nutrient-rich waste streams, such as anaerobic digester supernatants [[21],[24]] and RO permeates [[22],[25]]. For instance, Mondor et al. [26] and Ippersiel et al. [27] respectively obtained NH_4^+-N concentrates of 16 g L^{-1} and 21.35 g L^{-1} from swine manure by applying a batch ED system. In another work, Shi et al. [28] demonstrated the feasibility of nutrient recovery from pig manure by employing an ED system using bipolar membranes. Further, a pilot-scale demonstration (with seven months of operation) was shown by De Paepe et al. [29] that combined precipitation, nitrification and ED in concentrating urine. The conventional ED system was also applied to recover phosphate (~95.8%) from excess sludge solutions by Wang et al. [30] in continuous operation. Therefore, these studies may not provide an accurate assessment of ED performance in municipal wastewater (MWW) containing lower nutrient concentrations. Furthermore, MWW effluent has a low nutrient concentration; however, it can still deliver large nutrient loading to water resources due to the huge daily volume of wastewater released from wastewater treatment plants [31]. On the other hand, stringent nutrient discharge standards for treated wastewater effluent which mostly contains nitrate and phosphate pose a challenge with the currently used techniques, such as activated sludge and anaerobic/anoxic/oxic processes in wastewater treatment plants [32]. A conventional activated

sludge (CAS) system is an aerobic suspended biological nitrification process that converts ammonia into nitrite and nitrate via aerobic autotrophic bacteria, meanwhile reducing organic matter by microbial aggregates [33]. Therefore, nitrate is the most common mineral form of nutrient among nitrogen sources in CAS effluent [34].

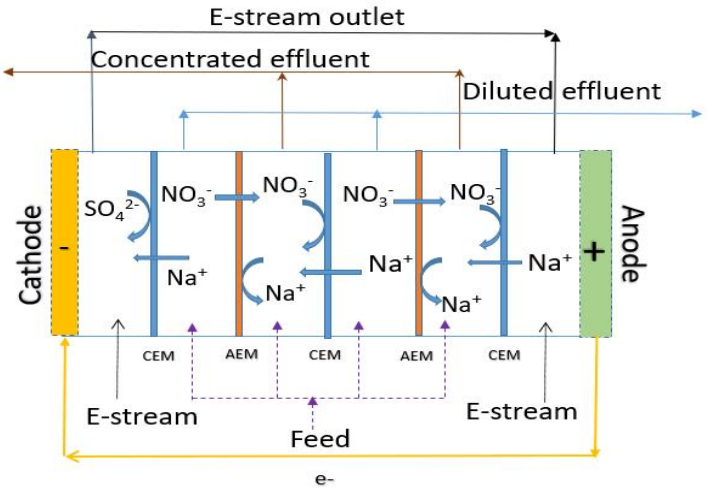

Fig. 1. *A schematic diagram of the ED system containing dilute, concentrate and electrolyte compartments separated by CEMs, AEMs and spacers. Electrolyte streams (E-streams) circulate within the electrode compartment.*

Two-thirds of the global population might suffer from the lack of fresh water by the year 2025, which will consequently increase the competition for water resources [15]. Meantime, 99% of MWW consists of water that has good potential for drinking water recovery [35]. Hence, the main focus of this work is separating and concentrating nitrate from the effluent of CAS to produce clean water with minimal or reduced energy and without any possible adverse environmental effect.

Therefore, in the first step, the impact of different operational parameters (limiting current density, water flow, operating time, the volume ratio of diluted to concentrated solution) was

investigated using synthetic wastewater. In the next step, the optimised ED system was validated for nitrate recovery using the effluent of the CAS process. Moreover, researchers have mainly focused on single-stage ED, and there is no research on nutrient recovery from wastewater with multi-stage ED. Therefore, the aim of this study is to enhance nitrate and water recovery with two-batch stage optimised ED systems. The water transfer rate through IX membranes, energy consumption, the selectivity of major counter ions and the fate of organic carbons as a probable challenge when using treated MWW were studied. Furthermore, the quality of diluted wastewater was tested for suitability to discharge to water bodies, as well as for its potential use as drinking water.

2. Materials and methods

2.1. Wastewater samples

In this work, we used both synthetic wastewater for the optimisation process and real wastewater to validate the ED process. Two different synthetic solutions were prepared with two different concentrations of nitrate, that is, with 150 mg L^{-1} and 500 mg L^{-1} from $NaNO_3$ salt in milli-Q water. A higher NO_3^- concentration was opted in this study in order to mimic the feed of second-stage ED in our study. In contrast, the low concentration used here simulates the NO_3^- concentration found in a real MWW stream. A broad range, from 50 to 500 mg L^{-1} NO_3^-, was applied for a limiting current density (LCD) experiment. The real MWW samples were collected during summer by using the grab sampling method from the secondary clarifier tank of the CAS system of Mikkeli wastewater treatment plant, Finland. The MWW in this experiment contained Cl^- (67.8 mg L^{-1} ± 0.42), NO_3^- (100 mg L^{-1} ± 10), SO_4^{2-} (113.3 mg L^{-1} ± 8), Na^+ (68.22 mg L^{-1} ±5.744), K^+ (33.55 mg L^{-1} ±3.38), Ca^{2+} (52.4 mg L^{-1} ± 6.3), total organic carbon (TOC; 10.19 mg L^{-1} ± 1.28) and total dissolved solids (TDS; 500 mg L^{-1} ± 12.9), with a pH of 6.6 - 7and salinity of 340 mg L^{-1} ± 9.94. Most freshwater lakes and streams have a

natural pH. Hence, changing the pH of the MWW discharge in an acidic and alkaline level can affect aquatic life. Therefore, working pH and the effluent pH were monitored thoroughly and considered as important parameters during the optimisation process in this study.

2.2. Lab-scale ED process design

Fig. 2a represents the primary single ED experimental setup in this study. The stack contained 10 cell pairs with an alternate CEM (Ralex CM-PES) and AEM (Ralex AM-PES) placed between the electrodes. The electrodes were made of platinum-coated with titanium in the effective size of 64 cm^2 per electrode. Similarly, the effective area of each membrane was 64 cm^2, and consequently, the total effective surface of membranes was 1344 cm^2. Both CEMs and AEMs were manufactured by Mega a.s. (Strazˇ pod Ralskem, Czech Republic); further information on the membranes can be found in the **Supplementary Material (Table S1).**

The polyethylene flow mesh spacers (thickness: 0.8 mm) separate the IX membranes and direct the flow of water across the membrane. As shown in **Fig. 2.a**, the similar feed used for the concentrate compartment (2000 mL volume) and the dilute compartment (with the initial working volume of 2000 mL), and 250 mL of 0.1 M Na_2SO_4 was used as an electrolyte solution. Two peristaltic pumps with a total of four heads circulated the solutions from inlet to outlet throughout the membranes, maintaining a uniform flow rate of 60 Lh^{-1}. The chemicals were purchased from Sigma Aldrich and Merck and were of analytical grades. The experiments were carried out in constant voltage mode (1–10 V; 1 V/cell pair) using a MASTECH HY3005D power supply. The equivalent current was read directly from indicators on the power supply.

The ED was performed with two conditions: a single-stage and a two-batch stage. In the two-batch stage process **(Fig. 2.b)**, the concentrated wastewater of the first stage was introduced to the second stage as the input for both the dilute and concentrate compartments. Both stages were operated under the optimised condition of four cell pairs, with a volume ratio of *VD/VC*

= 2/0.5 L, a flow rate of 60 Lh^{-1} and the constant voltage of 6.6 V. The operation was stopped once the conductivity of the dilute solution decreased to similar conductivity of the wastewater (706 $\mu S\ cm^{-1}$) of the input of the first batch stage. The polarity of electrodes was switched after each experiment in order to have a balance of oxidation and a reduction of electrodes, consequently protecting the electrodes from likely corrosion and scaling. Samples were collected from the diluted, electrode and concentrated streams every 10 min and were subjected to further analysis to determine the NO_3^- concentration. The conductivity, TDS and pH values of all solutions, as well as the cell potential, were measured every 10 min. The potential water transport of the concentrated solution was monitored with a graduated cylinder while considering the volume changes after sampling.

2.3. Experiments

In order to determine the applied voltage and the LCD, the same feed solution passed through the membranes in a single-pass flow at a flow rate of 60 Lh^{-1}. However, the electrode rinse solution circulated through the system during the experiment and was discarded after each test. Different nitrate concentrations of 50, 150, 300 and 500 mg L^{-1} NO_3^- were passed through the system, and the cell voltage was scanned from 0 V and increased step-wise to 20 V (0 to 2 V/cell pair) for each concentration. The resulting current was recorded for each voltage.

The various optimisation experiments were conducted via applying single-stage ED in two steps. The first step was conducted to determine (1) the effect of the diluted-to-concentrated stream volume ratio (*VD/VC*), (2) the effect of the recirculation flow rate and (3) the effect of cell pairs. Two synthetic solutions with 150 and 500 mg L^{-1} NO_3^- concentration under voltage of 4 and 6.6 V respectively, with 0.1 M Na_2SO_4 as electrolyte rinse solution, the flow rate of 60 Lh^{-1} and operation time of 30 min were used for first-step experiments generally. The effect of *VD/VC* was investigated at the ratios of 2/2, 2/1 and 2/0.5. Further, the effect of recirculation flow rate was studied at 40, 60, 80 Lh^{-1}, while the flow rate of the electrolyte solution was fixed

at 60 Lh^{-1}. The effect of cell pairs was examined with 4, 7 and 10 cell pairs with similar operating conditions.

Then, the second step was conducted by using CAS effluent as a feed solution in order to determine the effect of both the electrolyte type and the competing ions present in wastewater on nitrate removal and recovery. For these purposes, CAS effluent was used as feed solution under 6.6 V, with V_D/V_C of 2/0.5 and with a flow rate of 60 Lh^{-1} during the operation time of 40 and 120 min. The effect of the electrolyte solution was tested via applying 0.1 M NaCl, Na_2SO_4, H_2SO_4 and $NaNO_3$ solutions.

2.4. Analytical methods

The monitoring of water salinity, pH, TDS and conductivity were performed by using a multi-parameter PCSTEster35 alongside temperature compensation. The concentrations of NO_3^- and other anions in the aqueous and wastewater samples were performed by IC SI-50 4E ion chromatography (column size: 4 mm ID250 mm; flow rate: 0.7 mL min^{-1}; detector: suppressed CD). The concentrations of cations in solution were measured by IC YS-50 ion chromatography (column size: 4.6 mm ID125 mm; flow rate: 1 mL min^{-1}; YS-G guard column). Furthermore, the TOC content in the untreated and treated samples was determined using a TOC-V series Shimadzu analyser. Membrane fouling was investigated from scanning electron microscopy (SEM) images (Hitachi, S-4800) and Fourier-transform infrared spectroscopy (FTIR; Bruker Vertex 70) spectra. For this purpose, the membranes were collected from ED after terminating the experiment and were dried at room temperature before characterisation tests.

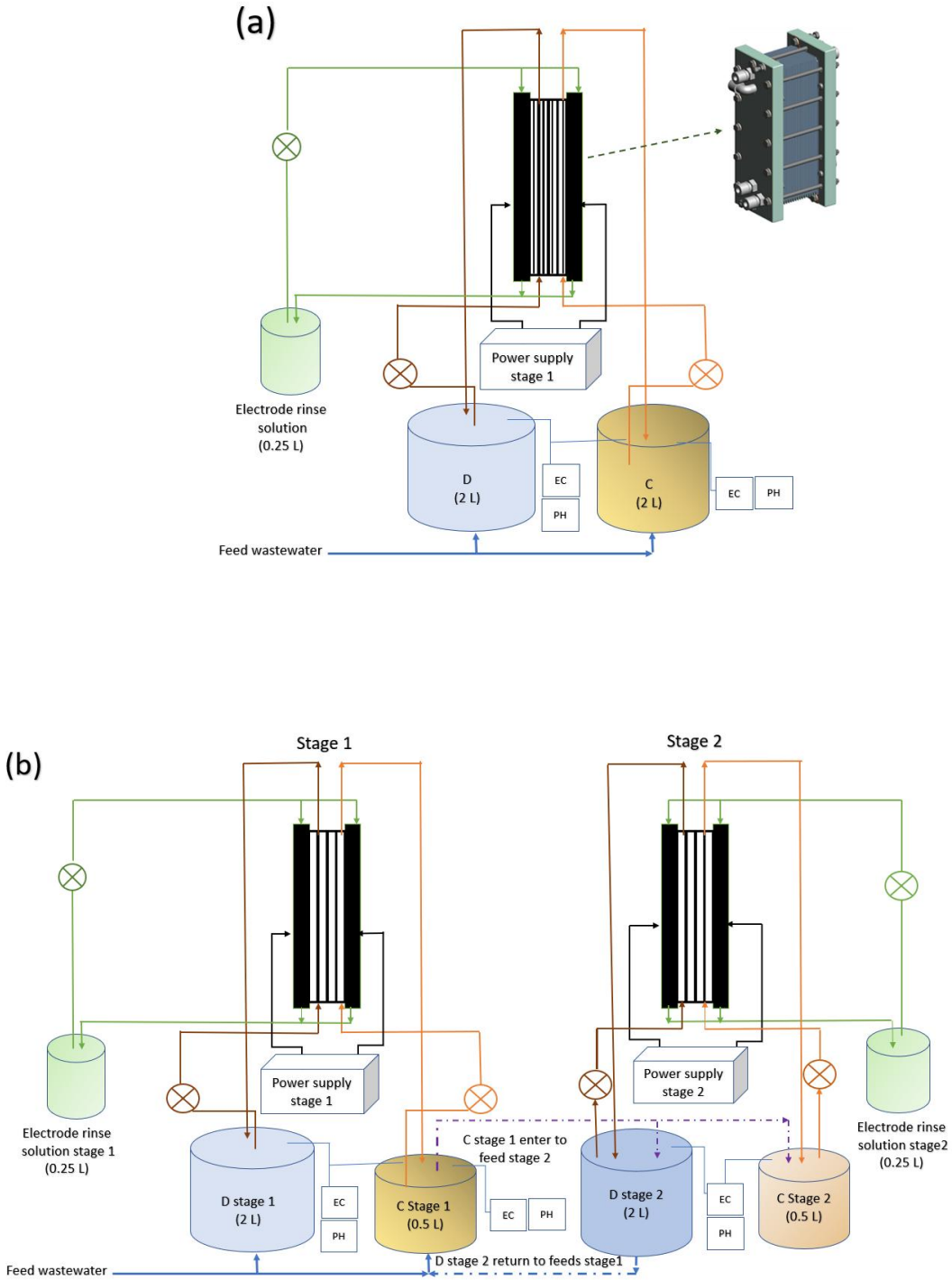

Fig. 2. *A schematic representation of the experimental setup: (a) the single-stage ED configuration (b) the two- batch stage ED configuration with concentrate solution of the first stage as the feed. D: dilute solution; C: concentrate solution; EC: electric conductivity and TDS meter.*

2.5. Data analysis

The hydraulic pump energy can be calculated by using **Equation (1.1)**:

$$P = \frac{Q \times H \times g \times \rho}{Pump\ efficiency(0.85)}, \quad (1.1)$$

where P is the hydraulic power (in W), Q is the flow capacity (in m^3s^{-1}), ρ is the density of the fluid (in kg m^{-3}), g is gravity (9.81 ms^{-2}), H is the differential head (in m) and the pump had 85% efficiency since pumps cannot work with full efficiency in reality [36]. The differential head was calculated based on the difference height level of the head pump and the discharge outlets in the ED setup.

The theoretical energy consumption ($E_{recovery}$) of the process that is required for the production of 1 kg of NO_3^- can be determined by using **Equation (1.2)**:

$$E_{recovery} = \int_0^t \frac{\mathrm{VI}}{(\mathrm{C}-\mathrm{C}_0)\times \mathrm{V}_\mathrm{C} \times 10^{-3}}\ \mathrm{dt}, \quad (1.2)$$

Where V is the voltage (in V), I is current (in amps), t is the ED operation time (in hr), (C-C_0) is the difference in nitrate concentration in the concentrated solution (in mg L^{-1}), V_C is the concentrated volume (in L), and 10^{-3} is the numerical coefficient for converting L to m^3 [[23],[37],[30]].

On the other hand, the theoretical energy consumption ($E_{removal}$) for the removal of 1 kg of NO_3^- can be determined by using **Equation (1.3):**

$$E_{removal} = \int_0^t \frac{VI}{(C0-C_t)\times V_D \times 10^{-3}}\ \mathrm{dt}, \quad (1.3)$$

where (C_0-C) is the difference in nitrate removal in the diluted solution (in mg L^{-1}) and V_D is the diluted volume (in L) [38]. It should be mentioned that the pumping energy consumption is not included in the theoretical energy consumption calculation.

The water transport (W, %) was calculated as:

$$W = \frac{V_{D,0} - V_{D,t}}{V_{D,0}} \times 100\%, \quad (1.4)$$

where $V_{D,0}$ and $V_{D,t}$ are the volumes of the dilute solution at times 0 and t respectively.

Further, the concentration ratio of the ED process was calculated simply via using **Equation (1.5):**

$$\text{Concentration ratio} = C_{C,t}/C_{D,0}, \quad (1.5)$$

where $C_{C,t}$ and $C_{D,0}$ are the concentration of concentrated solution, in mgL^{-1}, at time t and 0 respectively.

The mass value (in mg) obtained by dividing the concentration C_t to the volume of the solution V_t, at time t as:

$$\text{Mass} = C_t/V_t \quad (1.6)$$

3. Results and discussion

3.1. Optimisation of the ED system

3.1.1. Determining the applied voltage and LCD

One of the critical operating parameters in the ED process is the applied current or voltage, which majorly affect the process efficiency and the overall energy consumption of the process. A very low voltage or current can affect the ion migration across the chambers due to its weak driving force [[50],[51]].

Typically, along with increasing the voltage in the ED at a lower voltage, the current increases linearly, then the current increasing reduces and finally reaches a 'plateau', namely the LCD [39]; in this region the ion concentration at the membrane surface in the dilute cell approaches 0 and the electric resistance sharply increases due to ion depletion and the dissociation of water occurs, generating H^+ and OH^- ions, in order to generate ions [20]. The water dissociation

affects the current utilisation and can lead to a drastic pH value decrease in the dilute and an increase in the concentrate solution, which can, in turn, result in higher energy consumption and changes in solution pH. The pH changes can cause the precipitation of insoluble hydroxides on the membrane surface as well, leading to scaling [20]. When exceeding the limit for current and voltage, namely when over the LCD, the current does not increase, and thus resistances are changing drastically with the applied voltage [20]. Hence, establishing the LCD is of paramount importance in ED process optimisation in order to circumvent poor treatment efficiency and higher energy consumption.

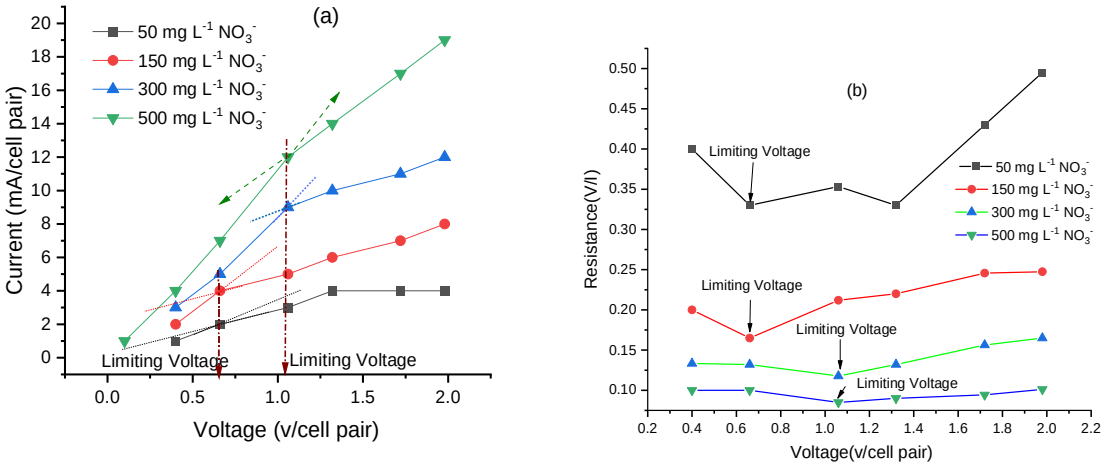

Fig. 3. *(a) Current voltage and (b) resistance voltage polarisation curves for nitrate solutions of different concentrations (with a flow rate of 60 L* h^{-1} *and 10 cell pairs).*

For this purpose, the graph of voltage–cell pair against the current–cell pair proposed by Isaacson and Sonin [39] is depicted in **Fig. 3.a.** The intersection of two extrapolated sloping lines represents the limiting current or voltage and can be found by extending the trend line of each graph, as shown in **Fig. 3.a.**

Other researchers have used the same method for this purpose [[40],[42],[43],[44]]. However, it is sometimes impractical to identify the slope changing point where the current density increases linearly as a function of voltage. A plot of voltage–cell pair against the current–cell pair could help to identify the slope change point for LCD estimation, as developed by Cowan and Brown [45].

The lowest point shows the LCD and equivalent voltage in this case, as shown in **Fig. 3.b**.

For the 150 mg L^{-1} NO_3^- that we used in this study, a linear increment in voltage was observed as the current density increased, identified as the ohmic region in **Fig. 3.a.** Above 0.66 mA/cell pair, a sharp decline in the slope was observed, suggesting increased resistance due to concentration polarisation or a depletion of ions in the membrane boundary layer. Meanwhile, in **Fig. 3.b,** increases the resistance observed at same current. Based on the intersection points in **Fig. 3.a**, a limiting current of 2, 4, 9, 12 mA was determined for the different concentrations of 50, 150, 300 and 500 mg L^{-1} NO_3^- respectively. The equal voltage for these limiting currents was 0.66 V/cell pair for 50–150 mg L^{-1} NO_3^- and 1.06 V/cell pair for 300–500 mg L^{-1} NO_3^-. **Fig. 3.b** also showed similar results. As suggested by the literature, 60% of the limiting voltage was considered as the safer operating voltage [[32],[36]]. As explained earlier, in practical LED operation, water splitting and depletion of ions in a diluted compartment might occur at the end of the operation time, applying limiting voltage or current. Therefore, for the following experiments, 4 and 6.6 V were used as the optimal voltages for two concentration ranges.

3.1.2. The effect of the diluted-to-concentrated volume ratio (V_D/V_C*)*

The objective of this experiment was to assess the possibility of obtaining a higher concentrated stream in a smaller volume of nutrient concentrated. Less volume in higher concentration will reduce the stages of ED processing and consequently, the operational cost. The effect of V_D/V_C was examined for both the cases of 150 and 500 mg L^{-1} NO_3^- concentrations via applying 4 and

6.6 V voltages respectively for an operating period of 30 min. The initial current was 20 and 80 mA for both the 150 and 500 mg L^{-1} NO_3^- concentration solutions and gradually decreased during the operation time (**Fig. S1** in the **Supplementary Material**). The NO_3^- concentration ratio of the product streams for various V_D/V_C are shown in **Fig.4**. TDS, salinity and EC were also checked here as indicators of the general performance of the ED.

It can be seen from **Fig. 4** that the improved NO_3^-, as well as overall TDS, were observed for V_D/V_C of 2/0.5, followed by V_D/V_C of 2/1 and 2/2, irrespective of the feed's NO_3^- concentrations. The nitrate concentration changed from 225 to 240 and 300 mg L^{-1}, along with increasing the concentrated volume from 2 to 1 and 0.5 L in 150 mg L^{-1} concentration. Likewise, the nitrate concentration increased from the initial of 500 to 800, 930, and 1300 mg L^{-1} in V_D/V_C 2/2, 2/1, and 2/0.5 respectively. Furthermore, the effect of V_D/V_C on synthetic wastewater quality and overall energy consumption (average value) of the process is listed in **Table 1**. In this work, we accomplished obtaining a residual NO_3^- concentration in the dilute compartment of about 65–80 mg L^{-1} for a process time of 30 min, higher than the discharge limit of 50 mg L^{-1} NO_3^-. By increasing the treatment time, the discharge NO_3^- standard could be met for the product stream containing NO_3^-. Changing the $V_{salt}/V_{acid\ or\ base}$ ratio from 1 (0.7/0.7) to 3 (2.1/0.7) in bipolar ED resulted in an increase in the concentration of the generated acid (HCl) and base ($NH_3 \cdot H_2O$) from 29.20 gL^{-1} and 26.25 gL^{-1} to 48.18 gL^{-1} and 43.05 gL^{-1} respectively [42]. Similar enhancements in the recovery efficiency were achieved by increasing the volume of the diluted solution in other literature [[28],[43],[44],[46]].

It can be seen from the table that the maximum energy consumption for recovery was found to be in the range of 0.26 to 0.54 $KWhKg^{-1}NO_3^-$ for the case of 150 mg L^{-1} and energy consumption of 0.33–0.75 $KWhKg^{-1}$ NO_3^-, obtained for the feed concentration of 500 mg L^{-1}. The higher resistance of 200 Ω was observed at a lower NO_3^- feed concentration of 150 mg L^-

[1], indicating the deficiency of the ions to migrate from diluted compartment toward concentrated compartment. With the increase in the NO_3^- concentration to 500 mg L^{-1}, the resistance value was reduced by two-fold (from average of 200 to average of 94. Ω). On further analysis of the data with respect to V_D/V_C, it can be understood that the lower energy consumption values were obtained for V_D/V_C of 2/2, followed by the ratios of 2/1 and 2/0.5; that is logical since the volume of concentrate compartment was in the denominator along with concentration difference (ΔC). Declined volume value dominated the concentration difference (ΔC) in energy consumption formula (Equation1.2). In similar studies by [30] and [44], the increase in energy consumption values was reported for an increase in V_D/V_C. Here the energy for nitrate removal is calculated for better comprehension. The energy consumption for nitrate removal decreased from the average amount of 0.60 to 0.54 and 0.47 KWh Kg^{-1} NO_3^- along, increasing the V_D/V_C from 2/2, to 2/1 and 2/0.5 in 150 mg L^{-1} NO_3^- respectively. Similarly, the energy consumption for nitrate removal decreased from about 0.63 to 0.62 and 0.6 KWh Kg^{-1} NO_3^- in V_D/V_C from 2/2, to 2/1 and 2/0.5 in 500 mg L^{-1} NO_3^- respectively.

Nevertheless, it should be realised that the better NO_3^- concentration ratio achieved in V_D/V_C of 2/0.5 among the three tested ratios and its energy demand for nitrate removal is the lowest. A higher volume of dilute also resulted in an increased number of ions migrating into the concentrate compartment [42] and consequently a decrease in the energy consumption for nitrate removal or separation. Further, a lower volume of concentrate will ultimately decrease the number of stages required for the further recycling and treatment of concentrate, making it more manageable and economical during the scaling-up of the ED process [42].

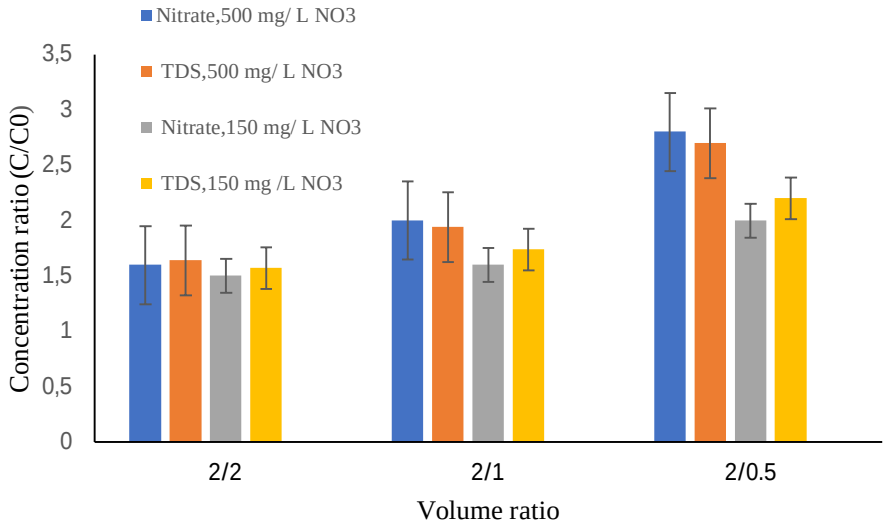

373

374 ***Fig. 4.*** *The concentration ratio of nitrate and TDS as a function of the volume ratio of diluted-*
375 *to-concentrated in 150 mg* L^{-1} NO_3^- *and 500 mg* L^{-1} NO_3^- *concentration (flow rate: 60* Lh^{-1}*;*
376 *operation time: 30 min; 10 cell pairs; voltage: 4–6.6 V).*

377 ***Table 1.****The effect of the diluted-to-concentrated volume ratio (*V_D/V_C*) on wastewater quality*
378 *and energy consumption.*

Volume ratio, V_D/V_C	**Energy consumption for recovery (KWh** Kg^{-1} NO_3^-**)**		**Nitrate Residual in dilute effluent (mg** L^{-1} NO_3^-**)**	
	C = 150 mgL^{-1} NO_3^-	C = 500 mgL^{-1} NO_3^-	C = 150 mgL^{-1} NO_3^-	C = 500 mgL^{-1} NO_3^-
2/2	0.28	0.33	80	130
2/1	0.35	0.53	77	125
2/0.5	0.53	0.74	65	116

379 Hence, there exists a trade-off between the treatment efficiency (i.e. the concentration ratio)
380 and overall energy consumption of the process. Based on these results, the V_D/V_C of 2/0.5 was
381 selected for the following studies in order to optimise other significant parameters of the
382 process. The hydraulic power pumping was about 0.25–0.26 W per pump in all experiments

for both concentrations. Since two pumps with two head pumps were used for circulating the solutions in this experiment, the estimated total hydraulic power pumping was about 0.5–0.56 W.

3.1.3. The effect of the recirculation flow rate

Contradictory statements can be found in the literature regarding the effect of the flow rate. Several works have reported the adverse effect of flow velocity on the separation of different ions [[46],[47],[48]]. Nevertheless, some studies have also shown the positive effects of the flow rate on ion removal [[47]]. The increase in flow rate can improve the ED performance by enhancing the mixing of the solution, decreasing the thickness of the diffusion boundary layer and increasing the diluted concentration on the membrane surface [[28],[48]]. As a result, the electrical resistance in the boundary layer would reduce, cause to improving ion removal. However, operating at a very high flow rate can result in reduced efficiency because the ions might not have enough time to pass through the membranes at higher feed velocities, causing an adverse effect on the rate of ion removal [[48],[60]]. Therefore, it is essential to investigate the optimum flow rate for an ED system in order to achieve the maximum NO_3^- recovery. In our study, the system is in batch mode means the dilute and concentrated solution circulates in the system for a certain time. For these tests, different recirculation flow rates of 40, 60 and 80 Lh^{-1} were assessed for the synthetic wastewater system containing an initial NO_3^- concentration of 150 mg L^{-1} and 500 mg L^{-1} with an electrolyte recirculation flow rate of 60 Lh^{-1}, the operation time of 30 min and the applied voltage of 4 and 6.6 V (with an average initial current of 20 and 80 mA for both 150 and 500 mg L^{-1} NO_3^- concentration solutions).

The NO_3^- and TDS concentration ratio for various flow rates can be viewed in **Fig. 5**. As can be seen in **Fig. 5, parts a and b**, the maximum NO_3^- concentration ratio were obtained at a recirculation flow rate of 60–80 Lh^{-1} for the feed NO_3^- concentrations of 150 and 500 mg L^{-1}.

In both concentrations, the recovery improved by increasing the flow rate from 40 to 60 Lh^{-1} due to more mixing effect and reducing the boundary layer near membranes. However, they were no noticeable increase in recovery efficiency when the flow rate increased to 80 Lh^{-1} and it seems that the flow higher than 80 Lh^{-1} will halt the recovery efficiency. The flow rate of 80 Lh^{-1} and higher would limit the retention time of ions to be transferred from one compartment to another through the membrane, and the ionic flux transport of salts decreases by the increase of the feed flow rates. Similarly, Fadel et al. [52] and Luo et al. [53] observed in their experiment that when the recirculating flow rate reached a certain value, ion migration almost ceased.

As expected from our previous observations, the NO_3^- concentration ratio increased with an increase in the feed's NO_3^- concentration of 150 to 500 mg L^{-1}. This trend is quite evident from **Fig. 5.c** where an enhanced TDS concentration ratio (from 2.66 to 3) was obtained when using 500 mg L^{-1} NO_3^- for a treatment period of 30 min. In contrast, this significant difference in TDS concentration ratio cannot be observed at 20 min with respect to NO_3^- feed concentrations since cations originated from the nitrate salt used here move simultaneously through IX which influence on TDS value. **Table 2** presented the average value of wastewater quality and energy consumption by the effect of recirculation flow rate. As can be seen from **Table 2,** the residual NO_3^- concentration in the produced water was also on a par with the standard discharge limit after 30 min when using a feed NO_3^- concentration of 150 mg L^{-1}. The average energy consumption values of 0.48–0.55 and 0.77–0.8 $KWhKg^{-1}NO_3^-$ were obtained at 60–80 Lh^{-1} for the feed NO_3^- concentration of 150 mg L^{-1} and 500 mg L^{-1} respectively. Based on these findings, a recirculation flow rate of 60 Lh^{-1} was opted in the recovery studies.

Furthermore, the average initial current was 20 and 80 mA for the applied voltage of 4 and 6.6 V for 150 and 500 mg L^{-1} NO_3^- concentration solutions respectively. As time progressed, the

current decreased due to depletion of ion in dilute solution (see **Fig. S2 in the Supplementary Material)**. Consequently, the ohmic resistance increased initially from 200 and 94.3 in 150 mg L^{-1} and 500 mg L^{-1} NO_3^- respectively.

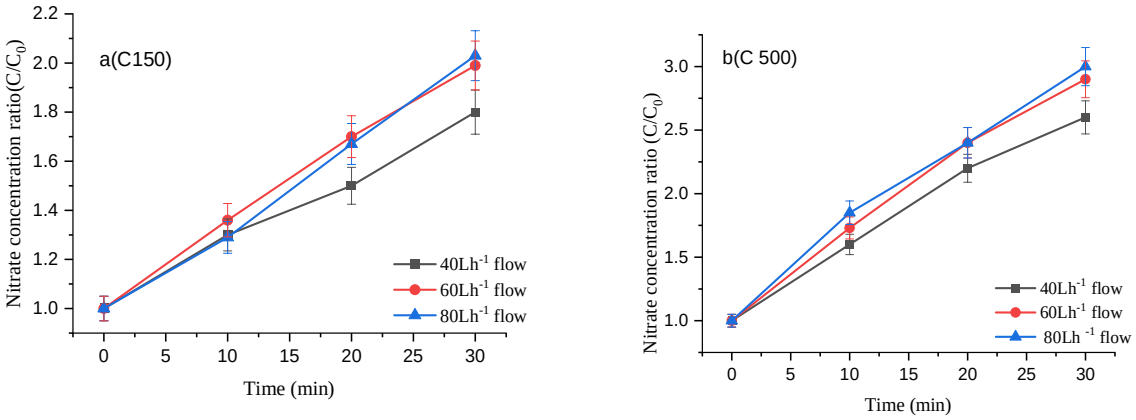

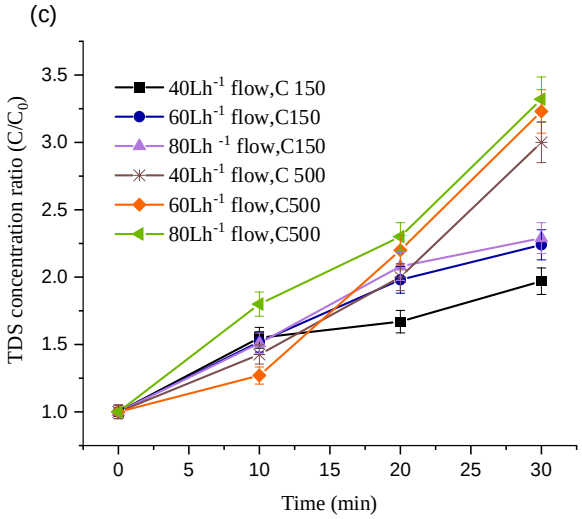

Fig. 5. *The NO_3^- concentration ratio as a function of the recirculation flow rate with (a) 150 mg L^{-1} NO_3^- concentration and (b) 500 mgL^{-1} NO_3^- concentration, and (c) the TDS concentration ratio as a function of the flow rate for both 150 and 500 mg L^{-1} NO_3^- concentrations (operation time: 30 min; 10 cell pairs; voltage: 4–6.6 V; V_D/V_C of 2/0.5).*

Table 2.*The effect of the recirculation flow rate on wastewater quality and energy consumption.*

Flow rate (Lh^{-1})	**The nitrate residual in dilute effluent (mgL^{-1} NO_3^-)**		**Maximum energy consumption for recovery ($KWhKg^{-1}$ NO_3^-)**	
	C = 150 mgL^{-1} NO_3^-	C = 500 mgL^{-1} NO_3^-	C = 150 mgL^{-1} NO_3^-	C = 500 mgL^{-1} NO_3^-
40	70	136	0.59	0.89
60	65	116	0.55	0.80
80	62	112	0.48	0.77

3.1.3. The effect of cell pairs

The stack design is one of the most relevant parameters for upscaling an ED system as the most significant part of the capital cost is associated with the cost of the membrane for the desired treatment capacity [54]. Therefore, the effect of 4, 7 and 10 cell pairs were examined over 30 min at a flow rate of 60 L h^{-1}. The experimental studies (**Fig. 6, parts a and b**) showed that 4 cell pairs displayed higher NO_3^- concentration ratio than 7 and 10 cell pairs. As expected, a higher NO_3^- concentration ratio of ~3.5 was obtained with an increase in the feed's NO_3^- concentration to 500 mg L^{-1}. **Table 3** shows the average value of wastewater quality and energy consumption by the effect of cell pairs number in ED. From **Table 3**, it can be observed that a decrease in membrane pairs (i.e. reduced stack thickness) improved the current consequently decreased the cell resistance and energy consumption, in which the effective membrane area decreased from 6.4 to 4.48 and 2.56 m^2 while reducing the cell pairs from 10 to 7 and 4 respectively. It seems that the positive effect of improving the electric current dominated on the likely adverse effect of reducing the membrane area in this experiment in terms of recovery efficiency. It should be considered that energy consumption base on the formula (**Equation1.2**)

is a function of several variables and generally increases with the concentration difference across the ED stack (ΔC) and declines with the product of current (I). Energy consumption values decreased along decreasing cell numbers since the concentration difference, and current values have changed simultaneously in our experiments **(Table 3).** Lower energy consumption was obtained in two compartments compared with the three compartments in the study of Li et al. [42]. Brauns [55] showed that the development of thinner membranes can give a significant enhancement of process performance. Further, there is a need to address the limitation concerning the stack design – that is, the number of cell pairs and the required membrane area – in the real pilot-scale ED unit demonstration in order to prevent high voltage drop. Therefore, the ED system with four cell pairs seems more suitable for the application in this study. **Fig. S3 in supplementary materials** shows the changes of current Vs time as a function of the number of cell pairs in 150 and 500 mgL^{-1} NO_3^- concentration.

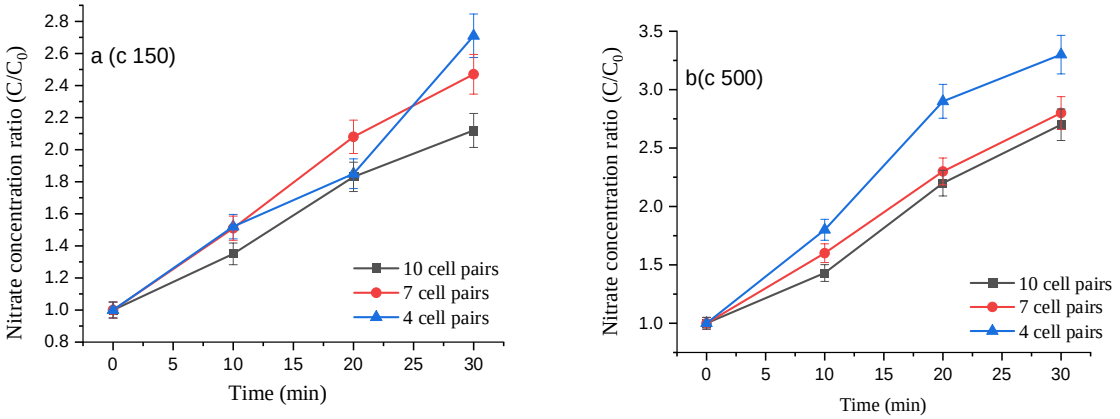

Fig. 6. *The NO_3^- concentration ratio as a function of the cell pairs for (a) 150 mg L^{-1} NO_3^- concentration and (b) 500 mg L^{-1} NO_3^- concentration (flow rate: 60 Lh^{-1}; operation time: 30 min;* V_D/V_C: *2/0.5).*

Table 3. *The effect of cell pairs on wastewater quality and energy consumption.*

Cell pair	**Initial current (mA)**		**Maximum resistance (Ω)**		**Nitrate residual in diluted effluent (mgL^{-1} NO_3^-)**		**Maximum energy consumption for recovery ($KWhKg^-$ NO_3^-)**	
	Voltage= 4 V *C* =150 mgL^{-1} NO_3^-	Voltage= 6.6 V *C*=500 mgL^{-1} NO_3^-	C= 150 mgL^{-1} NO_3^-	C = 500 mgL^{-1} NO_3^-	C = 150 mgL^{-1} NO_3^-	C = 500 mgL^{-1} NO_3^-	C = 150 mgL^{-1} NO_3^-	C = 500 mgL^{-1} NO_3^-
10	10	70	400	94	65	116	0.48	0.86
7	20	100	200	66	58	110	0.36	0.73
4	30	150	133	44	51	101	0.24	0.56

3.2. Validation with MWW

This step was performed using MWW collected from the secondary clarifier of CAS process. The optimised ED (flow rate: 60 Lh^{-1}; operation time: 30 min; 4 cell pairs; V_D/V_C: 2/0.5) based on the previous experiments made in this study was applied here.

3.2.1. The effect of the electrolyte type

The nature and concentration of electrolytes in the rinse stream play a vital role in electrode protection and, consequently, in their overall lifetime [56]. However, there is no explicit discussion available on the effect of electrolyte type on ED efficiency. Hence, in this study, we compared and evaluated ED performance on NO_3^- recovery and removal from MWW with a component, which is mentioned in the 'Materials and methods' section and shown in **Table 4**. The effect of 0.1 M NaCl, Na_2SO_4, H_2SO_4, and $NaNO_3$ electrode rinse solutions on the recovery efficiency of ED were tested. Overall, it can be understood from **Fig. 7** that Na_2SO_4 showed the highest nitrate recovery efficiency for the opted treatment time, followed by NaCl, H_2SO_4

498 and $NaNO_3$. Further, the difference in recovery efficiency was not significant between NaCl,
499 H_2SO_4, and $NaNO_3$ at the end of the experiment. Energy consumption for NO_3^- recovery with
500 our ED system using Na_2SO_4 as an electrolyte solution was determined to be 0.9 KWh Kg^{-1}
501 NO_3^-, recording the highest NO_3^- recovery efficiency and minimal energy consumption. After
502 the treatment period of 40 min, the concentration of NO_3^- in the dilute compartment decreased
503 to 25–30 ppm (below the discharge limit) in the dilute compartment, from an initial NO_3^-
504 concentration of ~110–150 mg L^{-1}, irrespective of the electrode rinse solution opted for in the
505 system. It is expected that the concentrating capacity could still improve with increased time.
506 Also, the leaching of NO_3^- from dilute and concentrate compartments into the electrode rinse
507 solution was found to be insignificant in all experiments. The pH of feed wastewater was about
508 (6.8-7.2) that increased slightly in concentrated wastewater (7-7.4) while it decreased slightly
509 in the dilute compartment (6.3-6.6) in all electrolytes experiments. According to Rotta et al.
510 [57] study, the depletion of ions in the diluted compartment at the end of operations might
511 exceed the limiting current density values, consequently lead to the concentration polarisation,
512 and generation of OH^- and H^+ by water splitting. The OH^- ions may pass through the membrane
513 to the concentrate side. However, in our experiment, pH changes were not significant, and it
514 started slightly from the beginning.

515 In contrast to other electrolytes in our study , with H_2SO_4 as the electrode rinse solution, the
516 pH dropped to 2.5 in the concentrated stream whereas the pH was found to be 4.3 in the diluted
517 stream. The significant pH drop in the concentrate stream could be the result of the rapid
518 migration of H^+ ions from the electrode rinse compartment to the neighbouring concentrate
519 compartment. Similar observations were also made in other works reported in the related
520 literature [[58],[57]]. However, during the extended operation time in the pilot-scale setup, a
521 low pH of H_2SO_4 as the rinse electrode might corrode the electrodes and the desirable limit of
522 the pH in the water discharged into the water reservoir should be considered to be 6.5–8.

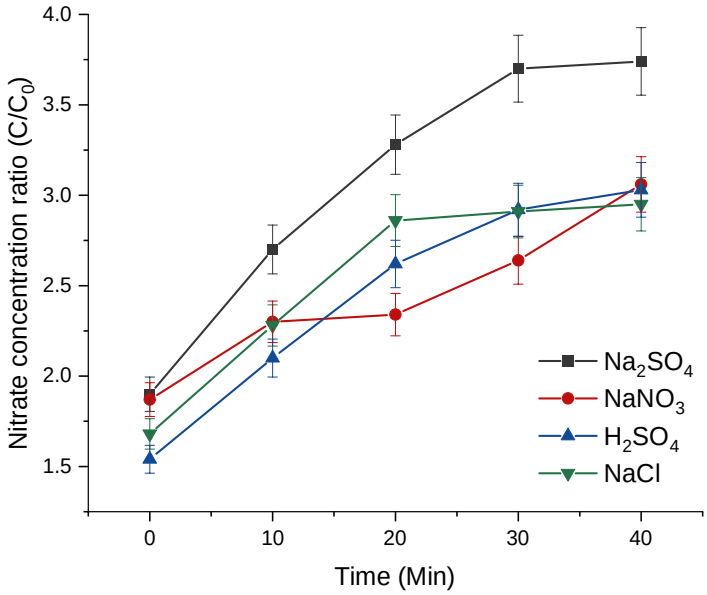

Fig. 7. *The NO_3^- concentration ratio as a function of the electrolyte rinse type in wastewater.*

3.2.2. The effect of competitive ions on nitrate removal and recovery efficiency

Municipal effluent typically contains other ions that can influence the removal and recovery of nitrate ions. The competition between the counter-ions in optimised conditions with Na_2SO_4 as the electrolyte rinse was also investigated and is presented in **Fig. 8** as a function of time. As shown in **Fig. 7**, other competing ions in wastewater (Na^+, K^+, Ca^{+2}, Cl^- and SO_4^{2-}) migrated along with NO_3^- under the influence of an electric field. Among these, the dominant ions were Cl^- and Na^+. In our study, we noticed that Cl^- and SO_4^{-2} competed strongly with NO_3^- and the selectivity of the anions can be arranged in the order of $Cl^- > NO_3^- > SO_4^{2-}$, which correlates with the general anion selectivity order of anion exchange and Hofmeister series ($I^- > (NO_3^- \sim Br^-) > NO_2^- > Cl^- > OH^- > SO_4^{2-} > F^-$) [59]. The selectivity of ion-exchange membranes for a specific ion can be caused by three different mechanisms:

1. The perm selectivity of ions is controlled with the same charge based on their hydrated size in an electrical field [[59],[60]]. Ions with smaller intrinsic crystal radii have a higher hydration number, larger hydrated radii and hold their hydration shells more strongly, which is more attractive for an IX membrane [61].
2. Ions with the same charge as the ions are rejected by a thin surface layer on the membrane [22].
3. In interactions among the ion-exchange fixed functional groups of the membrane and the mobile ions in solution, the fixed ion-exchange sites typically have higher attraction forces towards the multivalent counter-ions compared to monovalent ions [[22],[62]].

Our findings showed that the SO_4^{2-} ion demonstrated a slightly lower recovery in comparison to the other competitor anions. This could be attributed to the fact that the SO_4^{2-} has the largest hydrated ionic radius among the group and the size effect is dominant in this case since SO_4^{2-} has the lowest mobility [60]. Also, it should be mentioned that the ionic form of most AEMs and CEMs are Cl^- and Na^+ that exchange with other co-ion pollutants in the solution, so the higher concentration ratio of Cl^- and Na^+ in ED studies might be due to this phenomenon; however, no study mentioned this. Also, as seen in **Fig. 1,** Na^+ migration from the anodic Na_2SO_4 electrolyte compartment to the neighbouring concentrate compartment led to spurious judgment regarding membrane selectivity to Na^+. Besides, the ED process is influenced by both the electromigration force and ion-exchange selectivity. Therefore, the mobility of ions is dependent on the applied electrical field as well; a higher current or voltage can cause enhanced mobility of the multivalent cations and anions [62]. Van Der Bruggen et al. [63] observed the selectivity of $Cl^- > NO_3^- > SO_4^{2-}$ by Selemion and Tokuyama membranes in an ED system, similarly reported in this work.

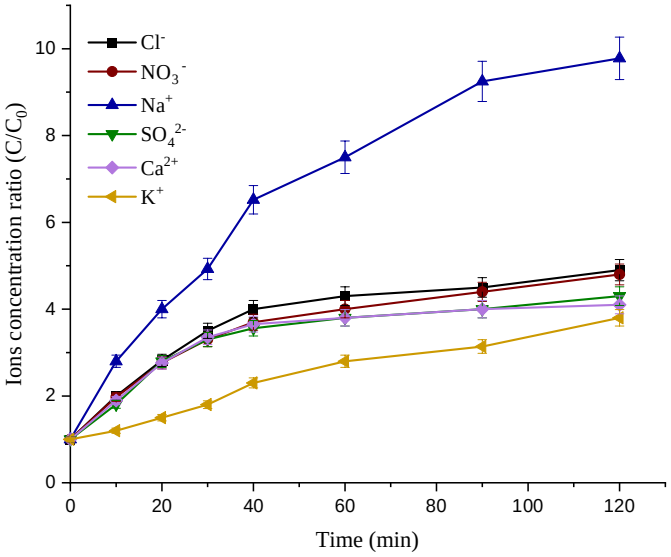

559

560 ***Fig. 8.*** *The concentration ratio of different ions in MWW effluent.*

561 *3.2.3. Enhancing recovery by multi-stage batch ED*

562 For this experiment, the system is designed as a two-batch stage system with interstage recycle
563 (see **Fig. 2**). In this case, the second-stage batch is used to produce a more concentrated product,
564 while the first-stage batch is used for freshwater production in the dilute compartment. The
565 average values of the characteristic of produced water and concentrated product are presented
566 in **Table 4**. **Fig. 9a** shows the salt concentration for the two-stages batch ED. The nitrate
567 concentration increased from the initial 100 to 460 (a concentration ratio of 4.6) and ultimately
568 to 1900 *mg* L^{-1} NO_3^- (a concentration ratio of 19) via applying first and second stage ED.
569 Similarly, the mass value in 0.5 L of the concentrated solution reached from the initial 50 to
570 230 and 1000 *mg* NO_3^- in first and second stage ED respectively **(Fig. 9.b).**

571 As shown in **Fig. 9.a**, the concentration ratio reduced somewhat as time progresses in both
572 stages. In the first stage, the recovery rate started from 4.8 mgL^{-1} per min and decreased to 0.03

573 mgL^{-1} per min at the ending of the process. Similarly, in the second stage, the recovery rate
574 declined from 15.5 to 1.3 mgL^{-1} per min as the time proceeds. This decreasing is due to
575 increasing the concentration gradient between the dilute and concentrated solutions caused by
576 osmosis phenomenon. In terms of nitrate standard, the time operation of 40 min could meet the
577 standard, and the second stage can be started from 40 min in functional ED. The concentration
578 ratio based on the mass was also decreased with the same rate **(Figs. 9.b)**.

579 Further, the overall current in the first-stage batch was lower than that in the second-stage batch
580 due to the low ion concentration in the first-stage batch. The current decreased as a function of
581 time owing to the decreasing ion concentration of the dilute (see **Fig. 9.c**). However, for the
582 second-stage batch, the current was higher, which is attributable to the higher concentration
583 that consequently decreased the resistance of the system and improved the current and ED
584 performance.

585 The energy consumptions were calculated in order to derive the total energy consumption for
586 the two-stage batch ED. Wastewater demanded 1.44 kWh kg^{-1} NO_3^- in a 120 min operation in
587 the first stage, and it slightly increased in the second stage to 2.9 kWh kg^{-1} NO_3^- as the current
588 increased. The total energy consumption for the two-stage batch ED was about 4.34 kWh kg^{-1}
589 NO_3^-. This shows the higher recovery efficiency of nitrate with low energy consumption in
590 comparison with the other state-of-the-art systems (see **Table 5**). Based on the drinking water
591 standards and in terms of energy-saving, 40–50 minutes of operation time in a single stage
592 could be adequate. As mentioned earlier total hydraulic power pumping per stage of ED was
593 0.5 Whr. Furthermore, for producing 0.5 L of concentrated nitrate (**Table 4**) 5 cycles of ED
594 in the first stage and 1 cycle of ED in the second stage is needed. For this purpose, a total of 3
595 Whr of hydraulic power pumping was consumed.

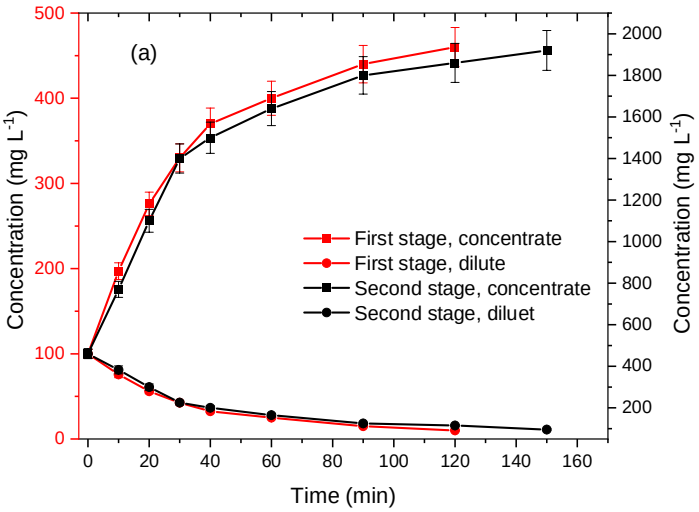

596

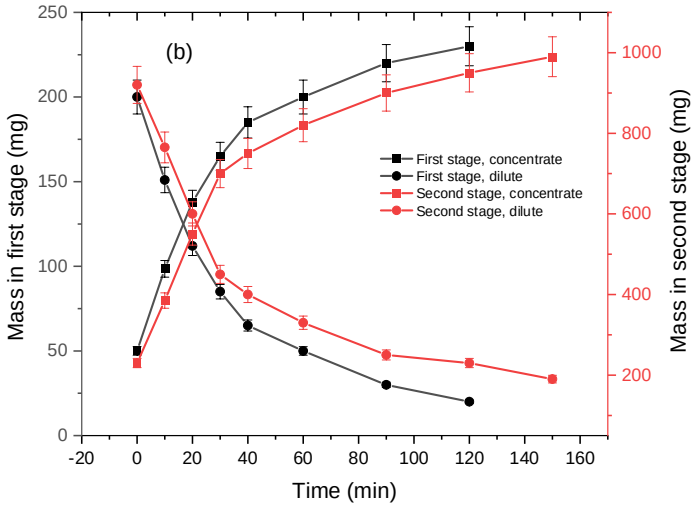

597

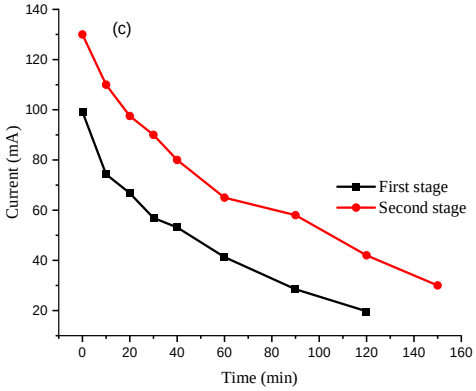

598

599

Fig. 9. *The effect of multi-stage batch ED on the (a) NO_3^- concentration (b)mass value and (c) current (flow rate: 60 Lh^{-1}; operation time: 120–150 min;* V_D/V_C*: 2/0.5; voltage: 6.6 V for each stage).*

Also, the water transportation phenomenon investigated here as a potential challenge during the ED concentrating process. Water molecules surrounded ions might pass with ions within the membrane from the dilute compartment to the concentrate compartment and consequently decreased the concentration of concentrated solutions and recovery efficiency. In general, water transport across an ion exchange membrane caused predominantly by electro-osmosis due to migration of hydrated ions under the gradient of electrochemical potential and also osmosis due to concentration difference[38]. However, compared with other ion-exchange membranes and other studies [38], the rate of water transfer in our system was low due to the type of membrane that was applied in the present study. The Ralex IX membranes are thicker than other commercial membranes and contain two dense polymeric substrates. The water transport in the second-stage batch was a little higher than that in the first-stage batch (10% in the first stage and 15% in the second stage) because more ions were transported to the concentrate compartment within the membrane.

622 ***Table 4*** *. Standards for potable water and chemical analysis of the potable water of Mikkeli*

623 *city, feed wastewater and ED diluted and concentrated product.*

624

Parameter	Table	Unit	World Health Organization	European Union	Potable water	Diluted product	Wastewater	Concentrated product (stage 1)	Concentrated product (Stage 2)
Aluminium	Al	mg L^{-1}	0.2	0.2	0.03	0	0.02	0.03	0.05
Cadmium	Cd	µg L^{-1}	3	5	0	0	0	0	0
Calcium	Ca	mg L^{-1}	100	100	56.92	0	52.4	208.48	835
Chromium	Cr	µg L^{-1}	50	50	0	0	0	0	0
Copper	Cu	mg L^{-1}	2	2	0.26	0	0.02	0.03	0.07
Iron	Fe	mg L^{-1}	0.3	0.2	0.03	0.03	0.12	0.06	0.08
Lead	Pb	µg L^{-1}	10	10	0	0.07	0.12	2.69	40
Magnesium	Mg	mg L^{-1}	30 -150	_	6.51	3.80	1.80	11	31
Nickel	Ni	µg L^{-1}	_	20	0	0.01	0.01	0.01	0.02
Nitrate	NO_3^-	mg L^{-1}	50	50	5.91	10	100	460	1920
Total dissolved solid	TDS	mg L^{-1}	500 - 1000	300	168	87.81	503	1740	8000
Electric conductivity	EC	µS cm-1 at 20°C	_	2500	234	124	706	2450	8502
Salinity	Sa	mg L^{-1}	_	_	113	59.40	340	1260	4669
pH	_	_	6.5 - 8.5	6.5 - 8.5	7	7.6	6.6 - 7	7.63	7.5
Phosphorus	P	mg L^{-1}	0	0	0	0.16	0.27	5.40	22
Total organic carbon	TOC	mg L^{-1}	_	_	3.71	6.32	10.19	16.32	25
Potassium	K	mg L^{-1}	20	_	15.20	1	33.55	127.30	381
Sulfate	SO_4^{2-}	mg L^{-1}	250	250	40.90	18.7	113.30	477.30	1908
Sodium	Na	mg L^{-1}	200	_	23	9.1	68.20	659.6	3000
Zinc	Zn	mg L^{-1}	0.01 - 3	5	0	0	0	0	0
chlorides	Cl	mg L^{-1}	250	250	25.40	6.8	67.81	332.7	1200

3.2.4. Products

The simultaneous production of clean water and liquid fertiliser were successfully achieved in our experiments. The product streams consisted of concentrated and diluted streams. It can be roughly estimated that 2 and 8 L of water will be recovered to produce 0.5 L of concentrated product in the single stage, which shows the high capability of water recovery from MWW by ED. The concentrated solution could be used as a liquid fertiliser in many applications; however, it needs the further separation of SO_4^{2-}, Na^+ and Cl^- ions for this purpose. The concentration of nitrate in the dilute compartment reached about 46 mg L^{-1} in 30 min with an effluent pH of near 7, which is suitable for discharge into water bodies (satisfying the discharge limit). Likewise, with the increase in treatment time, most of the ions were depleted to near zero by the end of the ED process in 120 min, as shown in **Table 4**. Even, the diluted product is of better quality than local potable water and standards regarding the measured components. However, the microbial quality was not checked as a part of this study. Hence, it must be checked to confirm its use as potable water. The TOC in diluted water was about 6.32 mg L^{-1}; this is higher in comparison with the TOC measured in potable water in this study. Activated carbon could be used as a pre- or post-treatment in ED to remove organic compounds, taste and odour.

655 ***Table 5***

656 *A comparison of this study's results with other studies.*

657

658

Types of wastewater	Methods	Number of membranes and effective area	Operation and conditions	Operation time (min)	Initial concentration	Concentration factor	Energy consumption	Ref.
Swine manure	Electrodialysis coupled with air stripping	10 cell pairs; AR204SZRA anionic membranes and CR67HMR cationic membranes; effective area: 220 cm^2 per membrane	Voltage: 17.5 V; 8 L of each volume; batch mode; dilute flow rate: 36 cm s^{-1}		3200 mg L^{-1} of TAN, 2500 mg L^{-1} K	7 TAN, 7 NH_4^+-N	18.05 k Wh kg-1 NH_4^+-N	[27]
Swine manure	Electrodialysis coupled with reverse osmosis	A combination of CMB/AMX membranes (Tokuyama Soda, Japan) and Cation 64 LMP/AR 103 QDP (Ionics, Watertown, MA, USA); effective area:100 cm^2; 3 cell pairs	10 EDs in batch modes; voltage: 1 V per membrane; current densities: <40 mA/cm^2	600	3.71 ± 2.45 to 5.54 ± 0.40 g L^{-1} NH_3–N	4.32 NH_3–N		[26]
Synthetic and real pig manure	Two-stage bipolar membrane ED	A heteregonus cation-exchange membrane, an anion-exchange membrane and a bipolar membrane (the Membrane company)	Current: 3 A; 4.1 L d^{-1} of dilute; 0.7 L d^{-1} of concentrate	330	187 mg L^{-1} PO_4^{3-}	9.48 PO_4^{3-}		[28]
Diluted human urine	Combining precipitation, nitrification and ED	10 cell pairs with standard PC SA AEMs and PC SK CEMs; effective area: 64 cm^2 per membrane	Voltage: 3.9 V, 1.8–2.1 L dilute; 0.5–2 L concentrate; current: 5 mA	480–840 min for dilute; 2880–4320 min for the concentrate	60 mmol L^{-1} in 20% urine and 115 mmol L^{-1} in 40% urine NO_3^- N; 0.75 mmol PO_4^{3-}	4.3 NO_3^--N, 2.6 PO_4^{3-}, 4.6 K		[29]

Synthetic excess sludge	ED (CED) and ED with bipolar membranes (EDBM)	Six membranes for CED; cation-exchange membrane (JCM-II-07) and an anion-exchange membrane (JAM-II-07); effective area: 99 cm^2; four membranes for EDBM (the NEOSEPTA company); effective membrane area of 7.07 cm^2	Conventional ED and 50 mA cm^{-2} for EDBM	CED: 300; EDBM: 130	100 mg L^{-} P	PO_4^{3-}: 4.2 CED; PO_4^{3-}: 15.5 in EDBM	CED: 5.3 kW h kg-1 H_3PO_4; EDBM: 29.3 k Wh kg^{-1} H_3PO_4)	[30]
RO concentrate	Standard and monovalent selective ion-exchange membranes	AEM: nonselective membrane, membrane selective for monovalent anions from PCA-Polymerchemie Altmeier GmbH and PCCell GmbH, (Heusweiler, Germany); five cell pairs; active surface area: 0.0064 m^2	Current densities: 46.9–78.1 A/m2; voltage: 24.5–75.0 V	300	Cl^{-1}:90, SO_4^{2-}:4.5 mmol L^{-1}	7 NH_4-N		[22]
Domestic anaerobic digester supernatant	Pilot-scale ED	A 30 cell pair pilot reactor with a 7.2 m^2 effective membrane area	Voltage: 30 V; current efficiency: 76 ± 2%; flow rate of 1250 mL min^{-1} (75 Lh^{-1}); 200 L recirculated concentrated and electrode; single-pass feed	4320	NH_4^{+1}-N: 835 ± 267 mgL^{-1}; K: 232 ± 41 mgL^{-1}	8 NH_4^{+}-N	5 k Wh kg NH_4^{+}-N	[24]
synthetic wastewater	Selective ED	3 cell pairs. CM,AM,MVA. effective surface:180cm^2 per membrane	Volumes 3L, batch mode; Current density 2.8(mA/cm^2).		0.32mmolL^{-1} NO_3^{-} ,0.43 mmol L^{-1} PO_4^{3-}-P	5 NO_3^{-}, 1.6 P		[64]

secondary effluent	selective electrodialysis	Batch mode, 3 cell pair, CM, AM , MVA. effective area 25 cm^2 per membrane	flow rate : 8 $mLmin^{-1.}$ Voltage: 5 V.	960	2 mgL^{-1} NO_3^--N, P	11 P, 20 NO_3^--N	1.85 kWhr m^{-3}	[32]
MWW	Batch ED	4 cell pairs; effective surface: 64 cm^2 per membrane	Voltage: 6.6 V; volume: 2 L dilute and 0.5 L concentrate; batch mode	120	100–150 mgL^{-1} NO_3^-	Single-stage: 4.6 , NO_3^-; two-stage: 19.2 NO_3^-	Single stage: 1.44 k Wh kg^{-1} NO_3^-; two-stage: 4.34 k Wh kg^{-1} NO_3^-	**Present study**

3.2.4. Fouling investigation

Different man-made activities result in the presence of dissolved organic carbon in MWW. Organic carbon is the energy substrate source for microorganisms and its consumption demands dissolved oxygen in water resources, which consequently threatens aquatic life [65]. Microorganisms are used for reducing organic components in the biological treatment of wastewater; however, the remaining organics might still create fouling challenges in the long operation of a membrane-based process, such as ED, which is used as tertiary treatment. The charged small organic matter (e.g. humic acids) that is present in wastewater can effect ED efficiency via blocking the pores, membrane functional groups and solution, leading to membrane fouling [22]. Fouling consequently increases the membrane resistance, which causes a decline in ion flux and the selectivity of the membrane [[19],[66],[67]].

AEMs are more susceptible to fouling when compared with CEMs since most organic components which transport the anions through the membranes are negatively charged [20]. TOC, determined as any organic carbon-containing compounds, was analysed here for both diluted and concentrated solutions (3 replicates) in ED in order to investigate the transport and

675 fate of organics. However, it must be noted that unlike raw wastewater effluents, the TOC
676 concentration was not found high in the feed wastewater used in this study. The TOC content
677 decreased from 10.19 ± 1.2 mg L^{-1} to an average of 6.32 ± 0.5 mg L^{-1} in the diluted stream in
678 120 min. At the same time, it increased to an average of 16.32 ± 1.5 mg L^{-1} and 25 ± 2 mg L^{-1}
679 in the concentrated solution after ED treatment in the first and second batch stages respectively.
680 The TOC results proved that the charged organic component transported from the dilute
681 compartment to the concentrate compartment. In Roman et al.[68]study, negatively charged
682 organic micropollutants were transported across the membraned due to Donnan dialysis. In
683 contrast, Fernadez et al. [69] did not observe TOC changing in both compartments due to the
684 large size of the hydrolysed polyacrylamide in his research.

685 The results from FTIR and SEM analysis are provided in the **Supplementary Material**
686 **(Figure S4, S5)**. The SEM image shows a thin layer of ion deposition and some bright spots
687 on the surface of the AEM in some areas, indicating signs (although not very distinct) of
688 probable fouling. Similarly, bright spots were observed on the CEM surface that represent the
689 slight fouling on the CEM. The following bands can be observed in all of the membranes: CH_2
690 scissor vibration (1470–1480 cm^{-1}), CH_2 (the polymer backbone) asymmetric and symmetric
691 stretching (2940 and 2860 cm^{-1}) and the stretching and scissor vibration of the OH group of
692 water (3400 cm^{-1} and 1640 cm^{-1}) [70]. The changing of bands in 1300–1400 cm^{-1} and between
693 600 and 1600 cm^{-1} might be due to organic fouling as the organic molecules have C-C and C-
694 H bonds within their structure in this range. Furthermore, a remarkable colour changing
695 observed in anion-exchange membrane side in contact with the concentrated compartment.

696 **4. Conclusion**

697 In this work, we have demonstrated the optimisation and enhancement of using an electrically
698 driven ED process for nutrient recovery in the form of nitrates from MWW. The optimisation

results showed that the higher nitrate recovery observed at the flow rate of 60 Lh^{-1}, V_D/V_C of 2/0.5, voltage of ~1 V/cell pair, four membrane cell pairs and 0.1 M Na_2SO_4 as the electrolyte solution. In the next step, the optimised ED was applied for nutrient recovery by two-batch stage ED. The studied ED method showed high recovery efficiency of NO_3^- (460 *mg* L^{-1} NO_3^- in the first stage and 1920 *mg* L^{-1} NO_3^- in the second stage) from the MWW collected from the secondary settling tank. More specifically, we achieved the low-energy consumption of ~1.44 kWh kg^{-1} NO_3^- in the first step and ~2.9 kWh kg^{-1} NO_3^- in the second step with our ED system. Eight litres of water could be recovered per 0.5 L of concentrated stream, indicating the high water recovery capacity of ED. The TOC results proved the transportation of organics from the dilute compartment to the concentrate compartment; however, no apparent fouling was observed by SEM. Overall, the nitrate concentrate obtained can be utilised as fertiliser after further treatment, while the diluted clean water can be used for secondary purposes.

Acknowledgments

The authors wish to acknowledge the financial support of this research by the European Regional Development Fund (ERDF) via the Regional Council of South Savo.

References:

[1] Bonn2011, The Water, Energy and Food Security Nexus - Solutions for a Green Economy, in: Policy Recomm., 2012.

[2] C.M. Mehta, W.O. Khunjar, V. Nguyen, S. Tait, D.J. Batstone, Critical Reviews in Environmental Science and Technology Technologies to Recover Nutrients from Waste Streams: A Critical Review Technologies to Recover Nutrients from Waste Streams: A Critical Review, Crit. Rev. Environ. Sci. Technol. (2015). doi:10.1080/10643389.2013.866621.

[3] T. Nur, W.G. Shim, P. Loganathan, S. Vigneswaran, J. Kandasamy, Nitrate removal using Purolite A520E ion exchange resin: batch and fixed-bed column adsorption modelling, Int. J. Environ. Sci. Technol. (2015). doi:10.1007/s13762-014-0510-6.

[4] N. Emami, A. Razmjou, F. Noorisafa, A.H. Korayem, A. Zarrabi, C. Ji, Fabrication of smart magnetic nanocomposite asymmetric membrane capsules for the controlled

release of nitrate, Environ. Nanotechnology, Monit. Manag. (2017). doi:10.1016/j.enmm.2017.09.001.

[5] E.A. Davidson, M.B. David, J.N. Galloway, C.L. Goodale, R. Haeuber, J.A. Harrison, R.W. Howarth, D.B. Jaynes, R.R. Lowrance, B. Thomas Nolan, J.L. Peel, R.W. Pinder, E. Porter, C.S. Snyder, A.R. Townsend, M.H. Ward, Excess nitrogen in the U.S. environment: Trends, risks, and solutions, Issues Ecol. (2011).

[6] R.W. Pinder, N.D. Bettez, G.B. Bonan, T.L. Greaver, W.R. Wieder, W.H. Schlesinger, E.A. Davidson, Impacts of human alteration of the nitrogen cycle in the US on radiative forcing, Biogeochemistry. (2013). doi:10.1007/s10533-012-9787-z.

[7] M. Maurer, W. Pronk, T.A. Larsen, Treatment processes for source-separated urine, Water Res. (2006). doi:10.1016/j.watres.2006.07.012.

[8] Y. Lin, M. Guo, N. Shah, D.C. Stuckey, Economic and environmental evaluation of nitrogen removal and recovery methods from wastewater, Bioresour. Technol. (2016). doi:10.1016/j.biortech.2016.03.064.

[9] W.A. Tarpeh, K.M. Udert, K.L. Nelson, Comparing ion exchange adsorbents for nitrogen recovery from source-separated urine, Environ. Sci. Technol. (2017). doi:10.1021/acs.est.6b05816.

[10] H. Huang, X. Xiao, B. Yan, L. Yang, Ammonium removal from aqueous solutions by using natural Chinese (Chende) zeolite as adsorbent, J. Hazard. Mater. (2010). doi:10.1016/j.jhazmat.2009.09.156.

[11] D.J. Batstone, T. Hülsen, C.M. Mehta, J. Keller, Platforms for energy and nutrient recovery from domestic wastewater: A review, Chemosphere. (2015). doi:10.1016/j.chemosphere.2014.10.021.

[12] E.M. Van Voorthuizen, A. Zwijnenburg, M. Wessling, Nutrient removal by NF and RO membranes in a decentralized sanitation system, Water Res. (2005). doi:10.1016/j.watres.2005.06.005.

[13] G. Adam, A. Mottet, S. Lemaigre, B. Tsachidou, E. Trouvé, P. Delfosse, Fractionation of anaerobic digestates by dynamic nanofiltration and reverse osmosis: An industrial pilot case evaluation for nutrient recovery, J. Environ. Chem. Eng. (2018). doi:10.1016/j.jece.2018.10.033.

[14] S. Sengupta, T. Nawaz, J. Beaudry, Nitrogen and Phosphorus Recovery from Wastewater, Curr. Pollut. Reports. (2015). doi:10.1007/s40726-015-0013-1.

[15] M.R. Esfahani, S.A. Aktij, Z. Dabaghian, M.D. Firouzjaei, A. Rahimpour, J. Eke, I.C. Escobar, M. Abolhassani, L.F. Greenlee, A.R. Esfahani, A. Sadmani, N. Koutahzadeh, Nanocomposite membranes for water separation and purification: Fabrication, modification, and applications, Sep. Purif. Technol. (2019). doi:10.1016/j.seppur.2018.12.050.

[16] E.U. Khan, Å. Nordberg, Membrane distillation process for concentration of nutrients and water recovery from digestate reject water, Sep. Purif. Technol. (2018). doi:10.1016/j.seppur.2018.05.058.

[17] L. Karimi, A. Ghassemi, How operational parameters and membrane characteristics affect the performance of electrodialysis reversal desalination systems: The state of the art, J. Membr. Sci. Res. (2016). doi:10.22079/jmsr.2016.20309.

[18] A. Campione, L. Gurreri, M. Ciofalo, G. Micale, A. Tamburini, A. Cipollina, Electrodialysis for water desalination: A critical assessment of recent developments on process fundamentals, models and applications, Desalination. (2018). doi:10.1016/j.desal.2017.12.044.

[19] M. Xie, H.K. Shon, S.R. Gray, M. Elimelech, Membrane-based processes for wastewater nutrient recovery: Technology, challenges, and future direction, Water Res. (2016). doi:10.1016/j.watres.2015.11.045.

[20] H. Strathmann, Electrodialysis, a mature technology with a multitude of new applications, Desalination. (2010). doi:10.1016/j.desal.2010.04.069.

[21] E. Thompson Brewster, A.J. Ward, C.M. Mehta, J. Radjenovic, D.J. Batstone, Predicting scale formation during electrodialytic nutrient recovery, Water Res. (2017). doi:10.1016/j.watres.2016.11.063.

[22] Y. Zhang, B. Van der Bruggen, L. Pinoy, B. Meesschaert, Separation of nutrient ions and organic compounds from salts in RO concentrates by standard and monovalent selective ion-exchange membranes used in electrodialysis, J. Memb. Sci. (2009). doi:10.1016/j.memsci.2009.01.030.

[23] W. Zhang, M. Miao, J. Pan, A. Sotto, J. Shen, C. Gao, B. Van der Bruggen, Separation of divalent ions from seawater concentrate to enhance the purity of coarse salt by electrodialysis with monovalent-selective membranes, Desalination. (2017). doi:10.1016/j.desal.2017.02.008.

[24] A.J. Ward, K. Arola, E. Thompson Brewster, C.M. Mehta, D.J. Batstone, Nutrient recovery from wastewater through pilot scale electrodialysis, Water Res. (2018). doi:10.1016/j.watres.2018.02.021.

[25] M. Reig, S. Casas, C. Aladjem, C. Valderrama, O. Gibert, F. Valero, C.M. Centeno, E. Larrotcha, J.L. Cortina, Concentration of NaCl from seawater reverse osmosis brines for the chlor-alkali industry by electrodialysis, Desalination. (2014). doi:10.1016/j.desal.2013.12.021.

[26] M. Mondor, L. Masse, D. Ippersiel, F. Lamarche, D.I. Massé, Use of electrodialysis and reverse osmosis for the recovery and concentration of ammonia from swine manure, Bioresour. Technol. (2008). doi:10.1016/j.biortech.2006.12.039.

[27] D. Ippersiel, M. Mondor, F. Lamarche, F. Tremblay, J. Dubreuil, L. Masse, Nitrogen potential recovery and concentration of ammonia from swine manure using electrodialysis coupled with air stripping, J. Environ. Manage. (2012). doi:10.1016/j.jenvman.2011.05.026.

[28] L. Shi, Y. Hu, S. Xie, G. Wu, Z. Hu, X. Zhan, Recovery of nutrients and volatile fatty acids from pig manure hydrolysate using two-stage bipolar membrane electrodialysis, Chem. Eng. J. (2018). doi:10.1016/j.cej.2017.10.010.

[29] J. De Paepe, R.E.F. Lindeboom, M. Vanoppen, K. De Paepe, D. Demey, W. Coessens, B. Lamaze, A.R.D. Verliefde, P. Clauwaert, S.E. Vlaeminck, Refinery and concentration of nutrients from urine with electrodialysis enabled by upstream precipitation and nitrification, Water Res. (2018). doi:10.1016/j.watres.2018.07.016.

[30] X. Wang, Y. Wang, X. Zhang, H. Feng, C. Li, T. Xu, Phosphate recovery from excess sludge by conventional electrodialysis (CED) and electrodialysis with bipolar

membranes (EDBM), Ind. Eng. Chem. Res. (2013). doi:10.1021/ie4014088.

[31] R.O. Carey, K.W. Migliaccio, Contribution of wastewater treatment plant effluents to nutrient dynamics in aquatic systems, Environ. Manage. (2009). doi:10.1007/s00267-009-9309-5.

[32] R. Liu, Y. Wang, G. Wu, J. Luo, S. Wang, Development of a selective electrodialysis for nutrient recovery and desalination during secondary effluent treatment, Chem. Eng. J. (2017). doi:10.1016/j.cej.2017.03.149.

[33] H. Eom, ScholarWorks @ UMass Amherst Investigation of Effluent Nitrogen Derived from Conventional Activated Sludge (CAS) and Biological Nutrient Removal (BNR) Systems and Its Impact on Algal Growth in Receiving Waters, (2016).

[34] J. Kim, M.J. Hwang, S.J. Lee, W. Noh, J.M. Kwon, J.S. Choi, C.M. Kang, Efficient recovery of nitrate and phosphate from wastewater by an amine-grafted adsorbent for cyanobacterial biomass production, Bioresour. Technol. (2016). doi:10.1016/j.biortech.2016.01.055.

[35] U.N.W.W.A. Programme, The United Nations World Water Development Report 2017: Wastewater, The Untapped Resource., J. Chem. Inf. Model. (2017). doi:10.1017/CBO9781107415324.004.

[36] M. Milnes, The mathematics of pumping water, R. Acad. Eng. (2000).

[37] Z.L. Ye, K. Ghyselbrecht, A. Monballiu, L. Pinoy, B. Meesschaert, Fractionating various nutrient ions for resource recovery from swine wastewater using simultaneous anionic and cationic selective-electrodialysis, Water Res. (2019). doi:10.1016/j.watres.2019.05.085.

[38] H. Yan, Y. Wang, L. Wu, M.A. Shehzad, C. Jiang, R. Fu, Z. Liu, T. Xu, Multistage-batch electrodialysis to concentrate high-salinity solutions: Process optimisation, water transport, and energy consumption, J. Memb. Sci. (2019). doi:10.1016/j.memsci.2018.10.008.

[39] X. Xu, Q. He, G. Ma, H. Wang, N. Nirmalakhandan, P. Xu, Selective separation of mono- and di-valent cations in electrodialysis during brackish water desalination: Bench and pilot-scale studies, Desalination. (2018). doi:10.1016/j.desal.2017.11.015.

[40] M. Ben Sik Ali, A. Mnif, B. Hamrouni, Modelling of the limiting current density of an electrodialysis process by response surface methodology, Ionics (Kiel). (2018). doi:10.1007/s11581-017-2214-7.

[41] T. Xu, Y. Zhang, W.Y. Zhao, M. Zhou, B. Yan, X. Sun, Y. Liu, Y. Wang, Waste conversion and resource recovery from wastewater by ion exchange membranes: State-of-the-art and perspective, Ind. Eng. Chem. Res. (2018). doi:10.1021/acs.iecr.8b00519.

[42] Y. Li, S. Shi, H. Cao, X. Wu, Z. Zhao, L. Wang, Bipolar membrane electrodialysis for generation of hydrochloric acid and ammonia from simulated ammonium chloride wastewater, Water Res. (2016). doi:10.1016/j.watres.2015.11.038.

[43] Y. Zhou, H. Yan, X. Wang, L. Wu, Y. Wang, T. Xu, Electrodialytic concentrating lithium salt from primary resource, Desalination. (2018). doi:10.1016/j.desal.2017.10.013.

[44] H. Yan, C. Xu, W. Li, Y. Wang, T. Xu, Electrodialysis to Concentrate Waste Ionic

Liquids: Optimization of Operating Parameters, Ind. Eng. Chem. Res. (2016). doi:10.1021/acs.iecr.5b03809.

[45] D.A. Cowan, J.H. Brown, Effect of Turbulence on Limiting Current in Electrodialysis Cells, Ind. Eng. Chem. (1959). doi:10.1021/ie50600a026.

[46] M. Ben Sik Ali, A. Mnif, B. Hamrouni, M. Dhahbi, Electrodialytic desalination of brackish water: Effect of process parameters and water characteristics, Ionics (Kiel). (2010). doi:10.1007/s11581-010-0441-2.

[47] Y. Kim, W.S. Walker, D.F. Lawler, Competitive separation of di- vs. mono-valent cations in electrodialysis: Effects of the boundary layer properties, Water Res. (2012). doi:10.1016/j.watres.2012.01.004.

[48] Y. Tanaka, Concentration polarization in ion-exchange membrane electrodialysis: The events arising in an unforced flowing solution in a desalting cell, J. Memb. Sci. (2004). doi:10.1016/j.memsci.2004.02.041.

[49] L. Karimi, A. Ghassemi, How Operational Parameters and Membrane Characteristics Affect the Performance of Electrodialysis Reversal Desalination Systems : The State of the Art Articles in Press Current Issue, J. Membr. Sci. Res. (2015).

[50] L.M. Camacho, J.A. Fox, J.O. Ajedegba, Optimization of electrodialysis metathesis (EDM) desalination using factorial design methodology, Desalination. (2017). doi:10.1016/j.desal.2016.07.028.

[51] Y. Zheng, X. Gao, X. Wang, Z. Li, Y. Wang, C. Gao, Application of electrodialysis to remove copper and cyanide from simulated and real gold mine effluents, RSC Adv. (2015). doi:10.1039/c4ra14328k.

[52] A. Fadel, R. Lafi, A. Aouni, A. Hafiane, S. Nacef, Separation of zinc ions from synthetically prepared brackish water using electrodialysis: effect of operating parameters, Desalin. Water Treat. (2016). doi:10.1080/19443994.2015.1086692.

[53] Z. Luo, D. Wang, D. Zhu, J. Xu, H. Jiang, W. Geng, W. Wei, Z. Lian, Separation of fluoride and chloride ions from ammonia-based flue gas desulfurization slurry using a two-stage electrodialysis, Chem. Eng. Res. Des. (2019). doi:10.1016/j.cherd.2019.05.003.

[54] H.J. Lee, F. Sarfert, H. Strathmann, S.H. Moon, Designing of an electrodialysis desalination plant, Desalination. (2002). doi:10.1016/S0011-9164(02)00208-4.

[55] E. Brauns, Salinity gradient power by reverse electrodialysis: effect of model parameters on electrical power output, Desalination. (2009). doi:10.1016/j.desal.2008.10.003.

[56] M.A. Menkouchi Sahli, M. Tahaikt, I. Achary, M. Taky, F. Elhanouni, M. Hafsi, M. Elmghari, A. Elmidaoui, Technical optimization of nitrate removal for groundwater by ED using a pilot plant, Desalination. (2006). doi:10.1016/j.desal.2005.06.025.

[57] E.H. Rotta, C.S. Bitencourt, L. Marder, A.M. Bernardes, Phosphorus recovery from low phosphate-containing solution by electrodialysis, J. Memb. Sci. (2019). doi:10.1016/j.memsci.2018.12.020.

[58] C. Casademont, M.A. Farias, G. Pourcelly, L. Bazinet, Impact of electrodialytic parameters on cation migration kinetics and fouling nature of ion-exchange

membranes during treatment of solutions with different magnesium/calcium ratios, J. Memb. Sci. (2008). doi:10.1016/j.memsci.2008.08.023.

[59] A. Elmidaoui, F. Elhannouni, M.A. Menkouchi Sahli, L. Chay, H. Elabbassi, M. Hafsi, D. Largeteau, Pollution of nitrate in Moroccan ground water: Removal by electrodialysis, Desalination. (2001). doi:10.1016/S0011-9164(01)00195-3.

[60] X. Wang, X. Zhang, Y. Wang, Y. Du, H. Feng, T. Xu, Simultaneous recovery of ammonium and phosphorus via the integration of electrodialysis with struvite reactor, J. Memb. Sci. (2015). doi:10.1016/j.memsci.2015.04.034.

[61] M.R. Awual, A. Jyo, Assessing of phosphorus removal by polymeric anion exchangers, Desalination. (2011). doi:10.1016/j.desal.2011.07.047.

[62] W. Jiang, L. Lin, X. Xu, H. Wang, P. Xu, Physicochemical and electrochemical characterization of cation-exchange membranes modified with polyethyleneimine for elucidating enhanced monovalent permselectivity of electrodialysis, J. Memb. Sci. (2019). doi:10.1016/j.memsci.2018.11.038.

[63] B. Van Der Bruggen, A. Koninckx, C. Vandecasteele, Separation of monovalent and divalent ions from aqueous solution by electrodialysis and nanofiltration, Water Res. (2004). doi:10.1016/j.watres.2003.11.008.

[64] Y. Zhang, S. Paepen, L. Pinoy, B. Meesschaert, B. Van Der Bruggen, Selectrodialysis: Fractionation of divalent ions from monovalent ions in a novel electrodialysis stack, Sep. Purif. Technol. (2012). doi:10.1016/j.seppur.2011.12.017.

[65] W.T. Mook, M.H. Chakrabarti, M.K. Aroua, G.M.A. Khan, B.S. Ali, M.S. Islam, M.A. Abu Hassan, Removal of total ammonia nitrogen (TAN), nitrate and total organic carbon (TOC) from aquaculture wastewater using electrochemical technology: A review, Desalination. (2012). doi:10.1016/j.desal.2011.09.029.

[66] J. Zhou, H. Kuang, W. Zhuang, Y. Chen, D. Liu, H. Ying, J. Wu, Application of electrodialysis to extract 5′-ribonucleotides from hydrolysate: Efficient decolorization and membrane fouling, RSC Adv. (2018). doi:10.1039/c8ra02550a.

[67] V. Lindstrand, G. Sundström, A.S. Jönsson, Fouling of electrodialysis membranes by organic substances, Desalination. (2000). doi:10.1016/S0011-9164(00)00026-6.

[68] M. Roman, L.H. Van Dijk, L. Gutierrez, M. Vanoppen, J.W. Post, B.A. Wols, E.R. Cornelissen, A.R.D. Verliefde, Key physicochemical characteristics governing organic micropollutant adsorption and transport in ion-exchange membranes during reverse electrodialysis, Desalination. (2019). doi:10.1016/j.desal.2019.114084.

[69] P.A. Sosa-Fernandez, J.W. Post, M.S. Ramdlan, F.A.M. Leermakers, H. Bruning, H.H.M. Rijnaarts, Improving the performance of polymer-flooding produced water electrodialysis through the application of pulsed electric field, Desalination. (2020). doi:10.1016/j.desal.2020.114424.

[70] A. Merkel, A.M. Ashrafi, M. Ondrušek, The use of electrodialysis for recovery of sodium hydroxide from the high alkaline solution as a model of mercerization wastewater, J. Water Process Eng. (2017). doi:10.1016/j.jwpe.2017.10.008.

Enhancement of nitrate removal and recovery from municipal wastewater through single- and multi-batch electrodialysis: Process optimisation and energy consumption

Rubaba Mohammadi [a *], Deepika Lakshmi Ramasamy [a], Mika Sillanpää [b,c,d,e]

[a]*Department of Separation Science, Lappeenranta-Lahti University of Technology, Sammonkatu 12, FI-50130 Mikkeli, Finland.*

[b] *Institute of Research and Development, Duy Tan University, Da Nang 550000, Vietnam.*

[c] *Faculty of Environment and Chemical Engineering, Duy Tan University, Da Nang 550000, Vietnam.*

[d] *School of Civil Engineering and Surveying, Faculty of Health, Engineering and Sciences, University of Southern Queensland, West Street, Toowoomba, 4350 QLD, Australia.*

[e] *Department of Chemical Engineering, School of Mining, Metallurgy and Chemical Engineering, University of Johannesburg, P. O. Box 17011, Doornfontein 2028, South Africa.*

[f] *School of Engineering Science, Lappeenranta-Lahti University of Technology, Lappeenranta 53851, Finland.*

[*]Corresponding author: Rubaba.Mohammadi@lut.fi, ru.mohammadi@ymail.com

Table S1: Main properties of ion exchange membranes

Properties	RALEX CM-PES	RALEX AM-PES
Ion-Exchange Group	$R–SO_3^-$	$R–(CH3)_3N^+$
Ionic Form, Counter Ion	Na^+	Cl^-
Basic Binder on Base	Polyethylene	Polyethylene
Fitting Fabrics	Polyester	Polyester
Thickness of Dry Membrane	<0.45	<0.45
Resistance in 0.5 M NaCl	<8	<7.5
Perm Selectivity	>90	>90

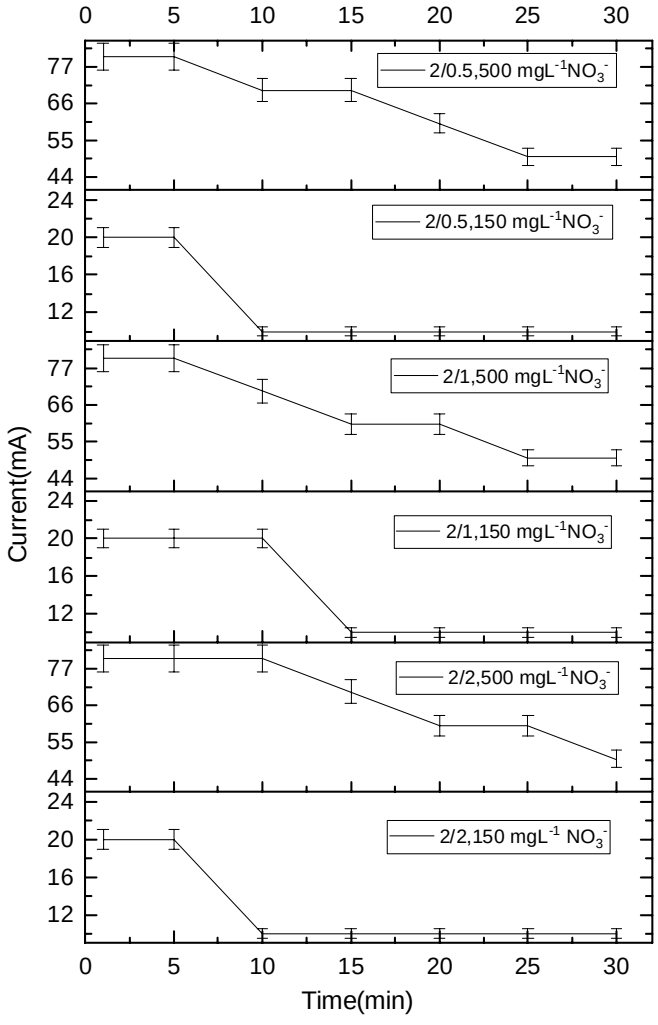

Fig. S1. Current vs. time changes as a function of the volume ratio of dilute to concentrate in (a) 150 and (b) 500 mg L^{-1} NO_3^- concentration (flow rate 60 Lh^{-1}, operation time 30 min, 10 cell pairs, voltage 4 - 6.6 V).

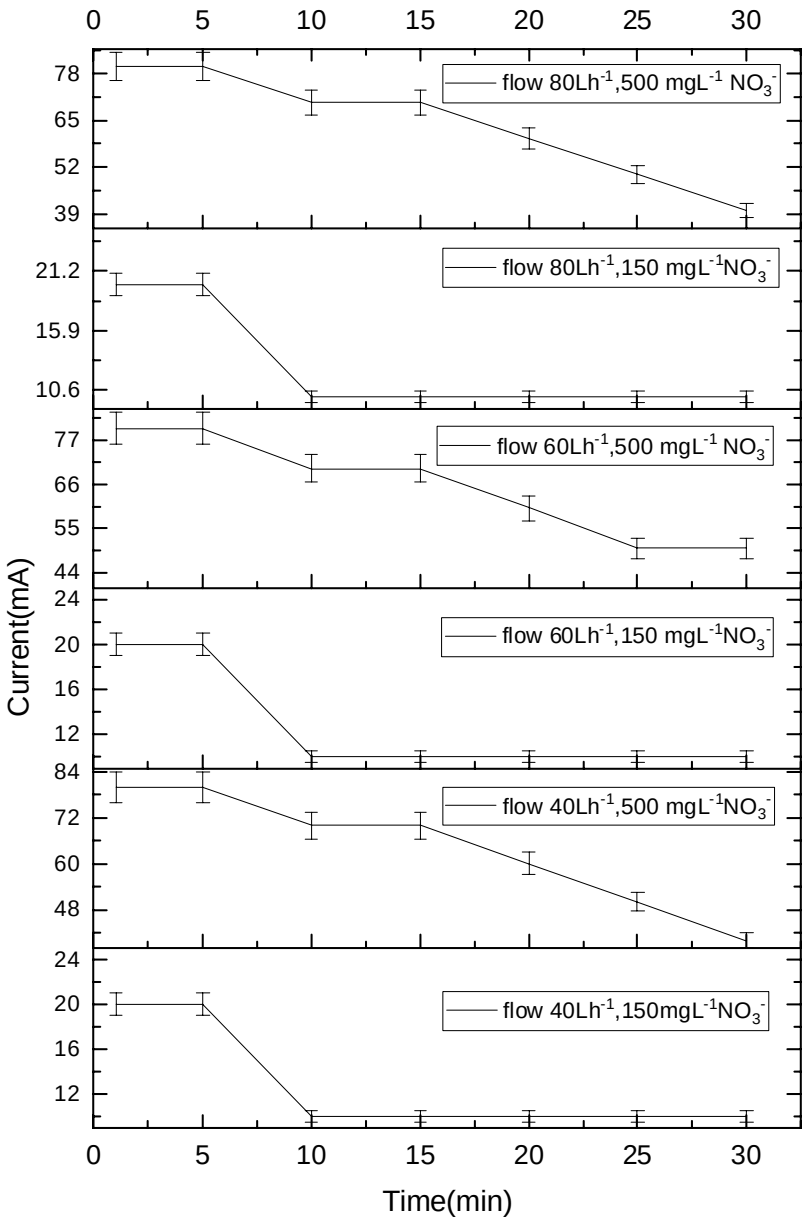

Fig. S2. The Current vs. time changes as a function of the flow rate in 150 and 500 mgL^{-1} NO_3^- concentration (operation time 30 min, 10 cell pairs, voltage 4-6.6 V, V_D/V_C of 2/0.5).

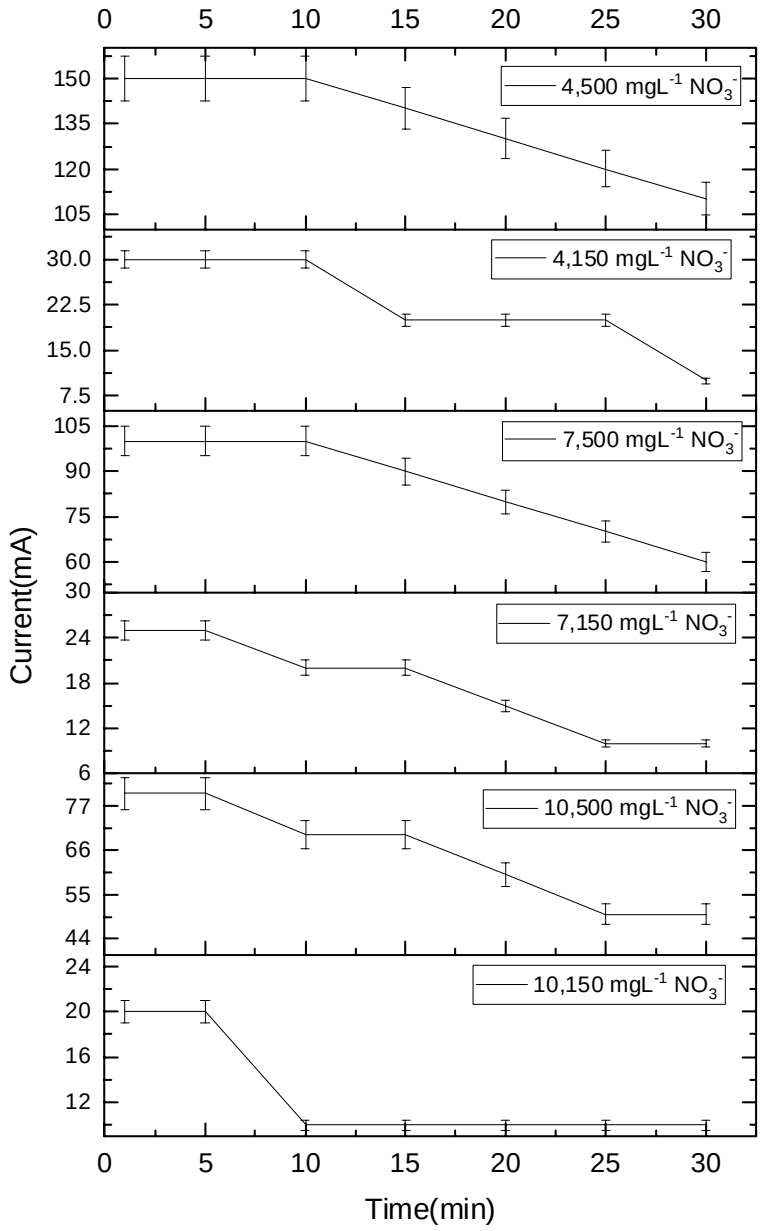

Fig. S3. The Current vs. time changes as a function of the number of cell pairs in 150 and 500 mgL^{-1} NO_3^- concentration (operation time 30 min, flow rate 60 Lh^{-1}, voltage 4-6.6 V, V_D/V_C of 2/0.5).

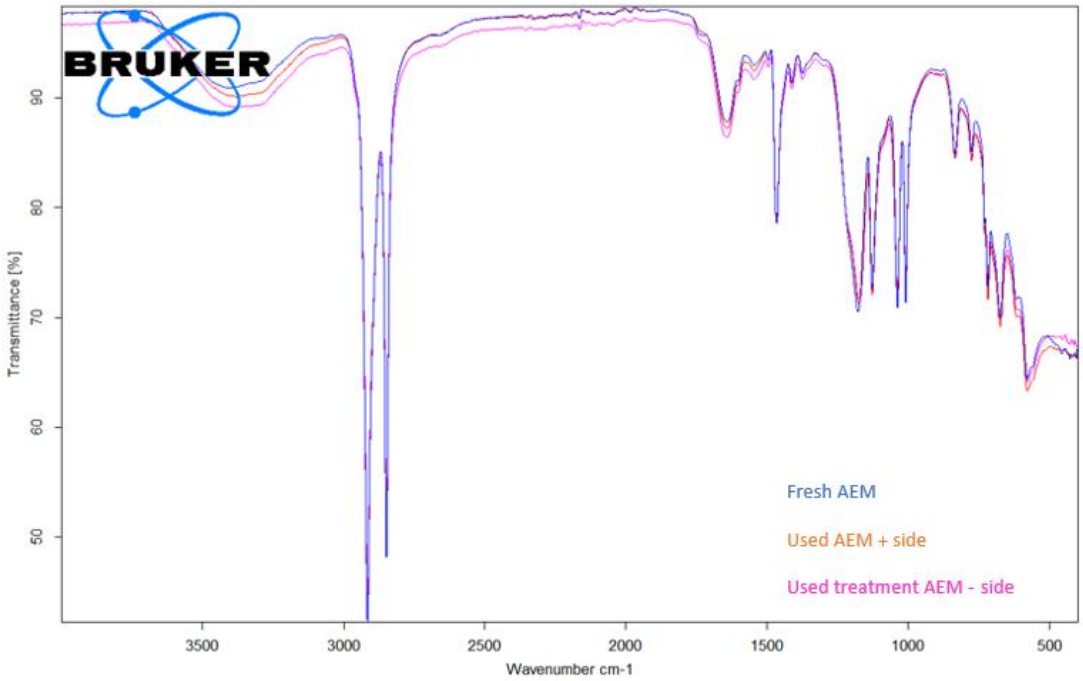

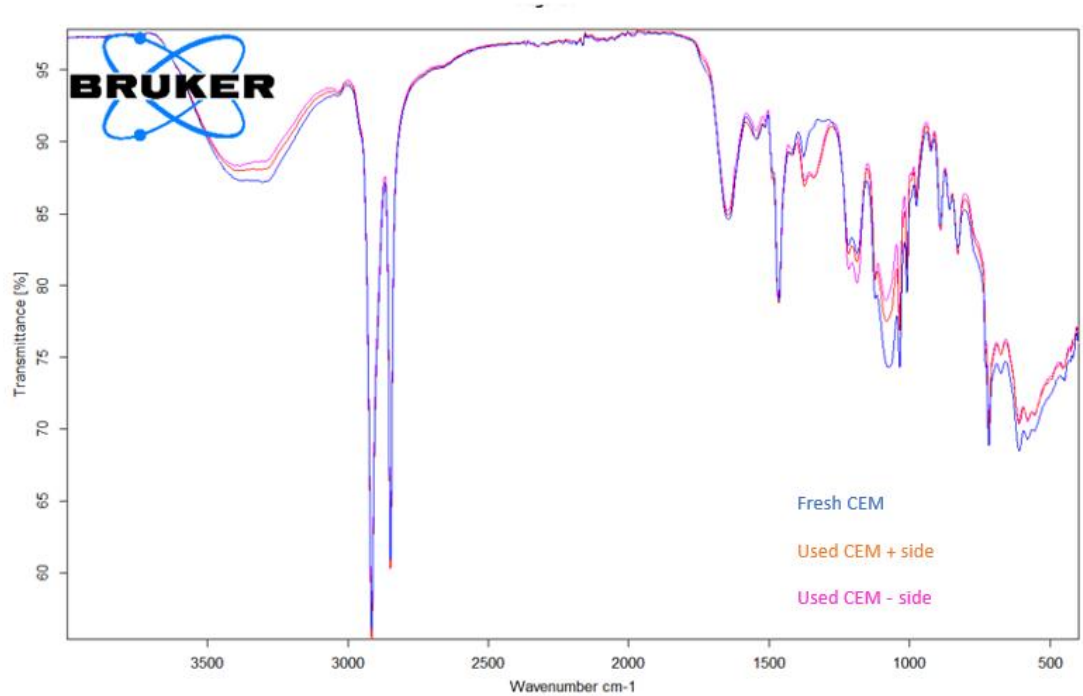

Fig. S4. ATR-FTIR spectra of fresh and used membrane

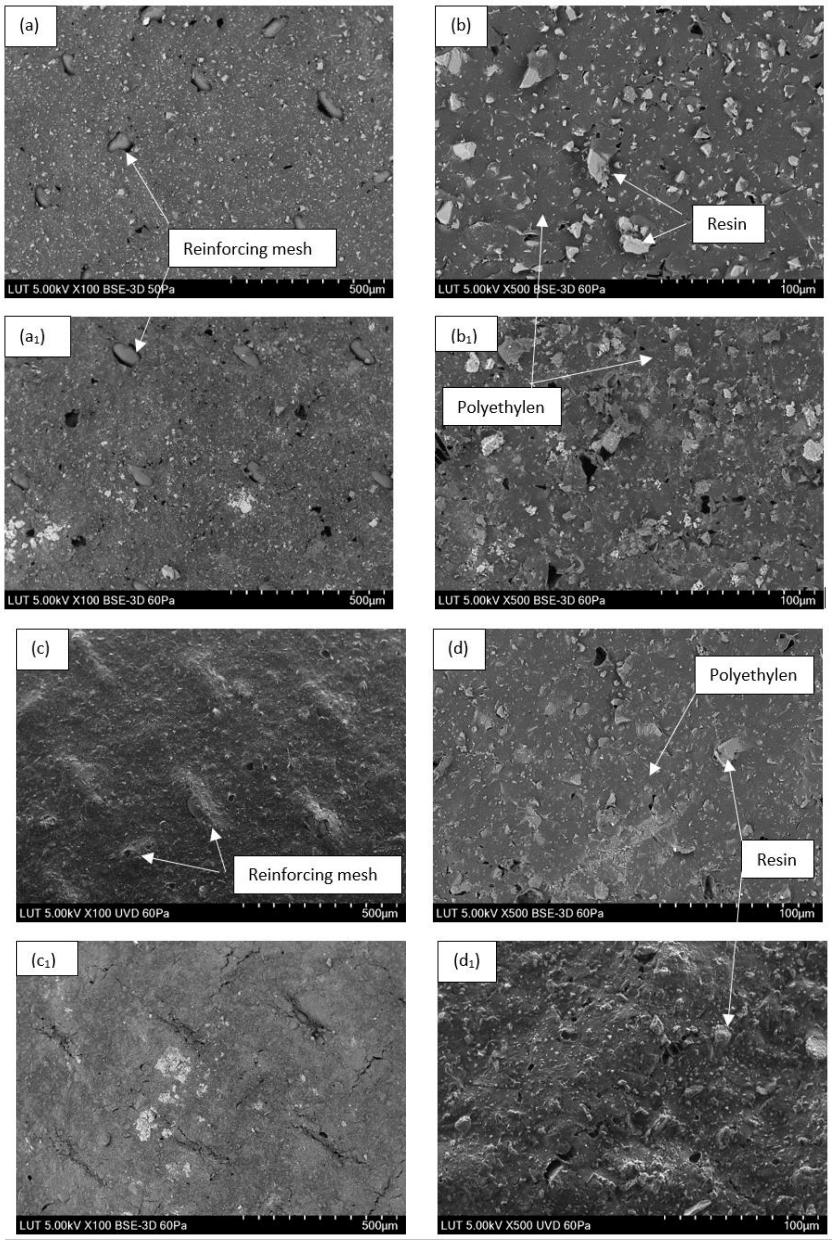

Fig. S5. Surface image of membrane(a,b):fresh surface of CEM ,(a1, ,b1):used surface of CEM,(c,d):fresh surface of AEM,(c1, ,d1):used surface of AEM